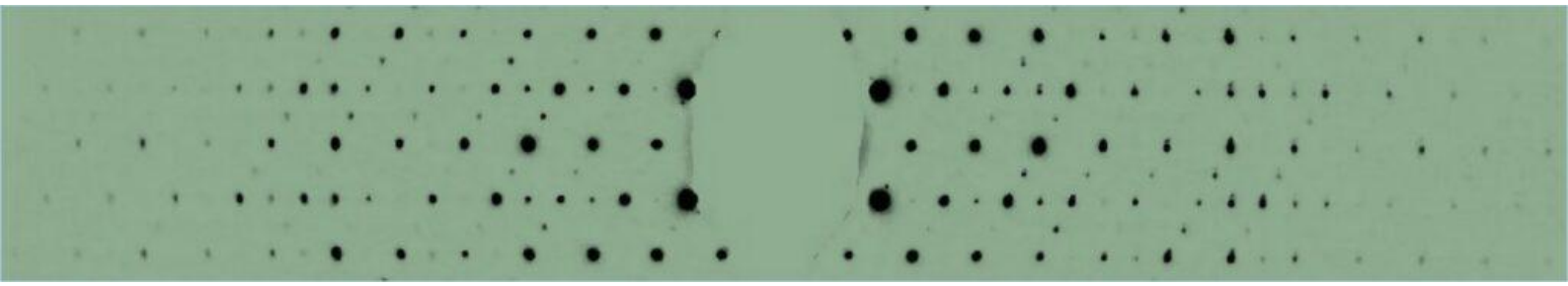

WiSe-Cryst 2026

Winter School on Electron Crystallography

March 2nd – 6th, 2026

Ernst Ruska-Centre | Forschungszentrum Jülich | Germany

Contact:
Program Contents: Dr. Tatiana Gorelik, t.gorelik@fz-juelich.de, +49 176 236 114 89
Event Management: Dr. Genevieve Wilbs, g.wilbs@fz-Juelich.de, +49 170 3855765

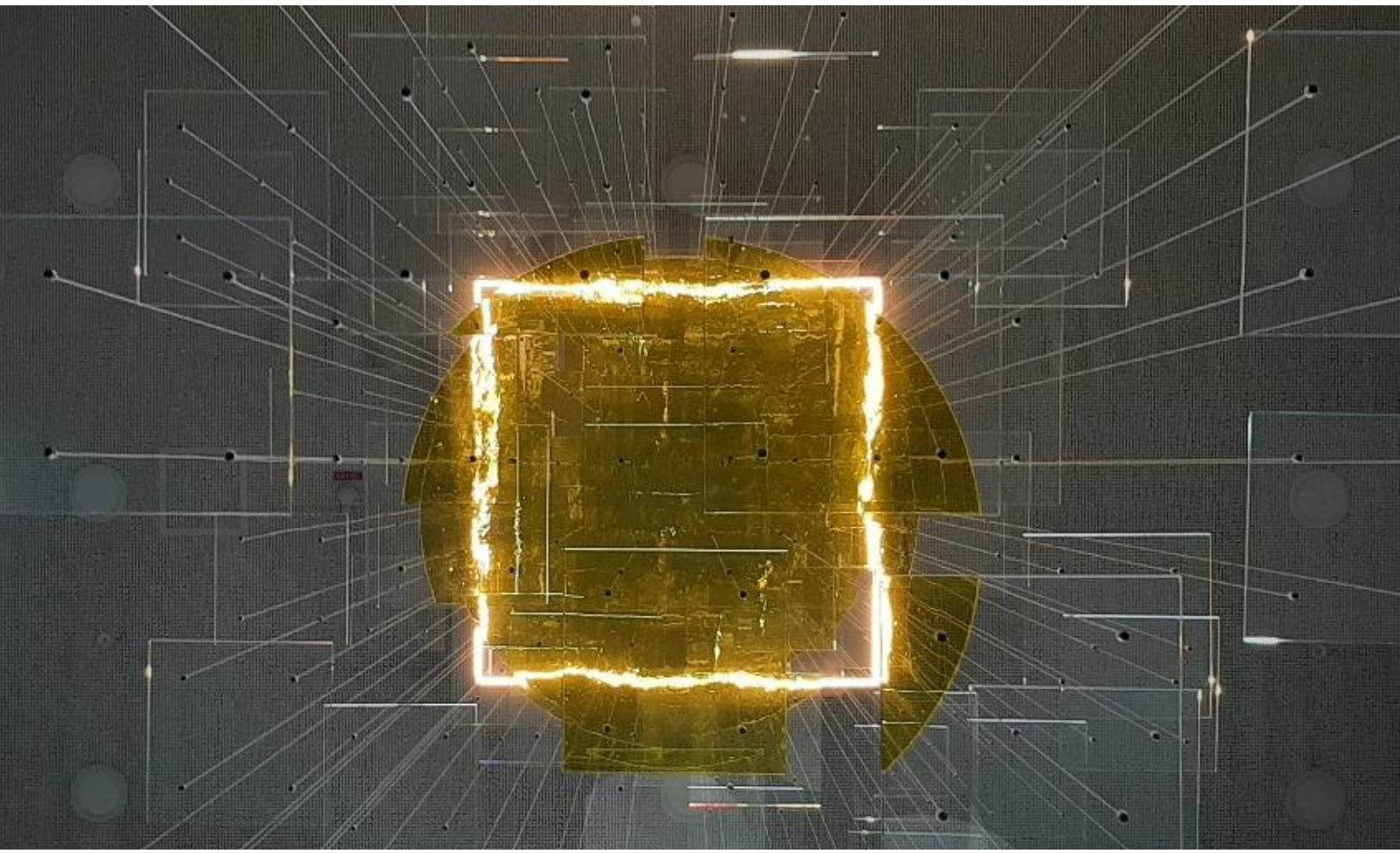

PRACTICAL INFORMATION

IMPORTANT

The Forschungszentrum Jülich Campus is **NOT OPEN TO PUBLIC** and access is regulated very strictly by our security service. Hence, please have **BOTH** your **access ticket** and a valid **Passport or ID card** with you **all the time.** Please also note, that taxis are not allowed on campus. In case you plan to travel by taxi, you will have to leave it at the gate and walk to the venue. Walking distance is 10-15 min.

CATERING

We will jointly have **lunch** in a separate room at the **canteen** (see campus map). The required lunch **tickets** will be handed out daily before lunch.
Coffee and the Welcome Reception will be provided in the **break area of building 05.13**.
The joint **dinner** will be served at the **TimberJacks** Restaurant in Düren. The shuttle bus will bring you there Thursday evening. Afterwards you can walk back to the B&B hotel. **Food and non-alcoholic drinks up to 50€ per person** is on us, but please do **leave a tip** for the waiters.

SHUTTLE BUS

During the event, a shuttle bus will bring you to the campus and back as follows:

Date	Time	Meeting Point	Destination
March 02	08:00 AM	In front of Hotel B&B	Forschungszentrum Jülich building 05.13
March 02	07:00 PM	Forschungszentrum Jülich building 05.13	Hotel B&B
March 03	08:00 AM	In front of Hotel B&B	Forschungszentrum Jülich building 05.13
March 03	05:30 PM	Forschungszentrum Jülich building 05.13	Hotel B&B
March 04	08:00 AM	In front of Hotel B&B	Forschungszentrum Jülich building 05.13
March 04	05:30 PM	Forschungszentrum Jülich building 05.13	Hotel B&B
March 05	08:00 AM	In front of Hotel B&B	Forschungszentrum Jülich building 05.13
March 05	05:30 PM	Forschungszentrum Jülich building 05.13	Restaurant TimberJacks Düren
March 06	08:00 AM	In front of Hotel B&B	Forschungszentrum Jülich building 05.13
March 06	02:15 PM	Forschungszentrum Jülich building 05.13	Düren Main Station & Hotel B&B

CAMPUS MAP

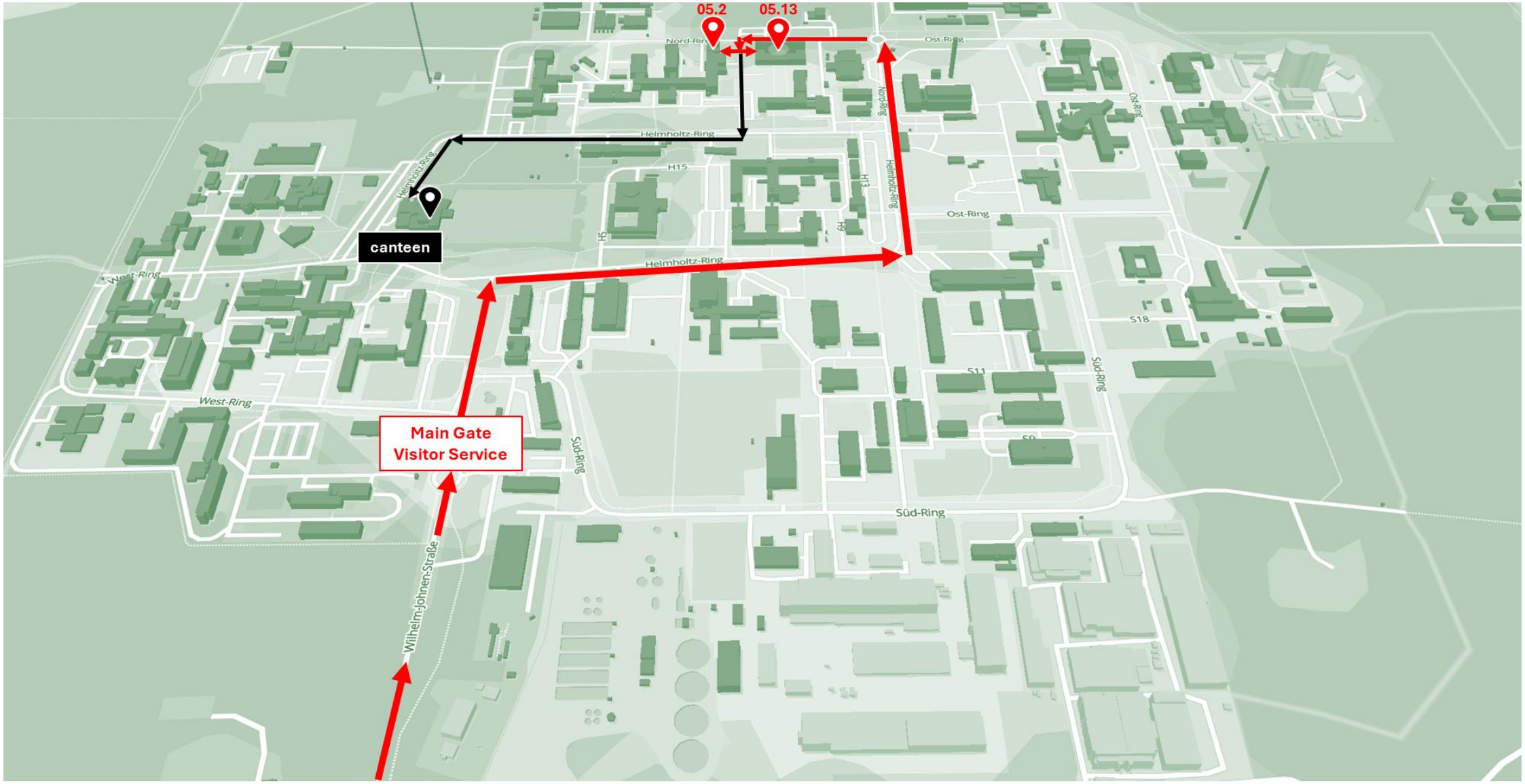
05.2
05.13
canteen
Main Gate
Visitor Service
Helmholtz-Ring
Ost-Ring
Süd-Ring
West-Ring
Nord-Ring
Wilhelm-Johnen-Straße
H15
H13
H9
H5
S18
S11

ER-C MAIN BUILDINGS

BUILDING 05.13

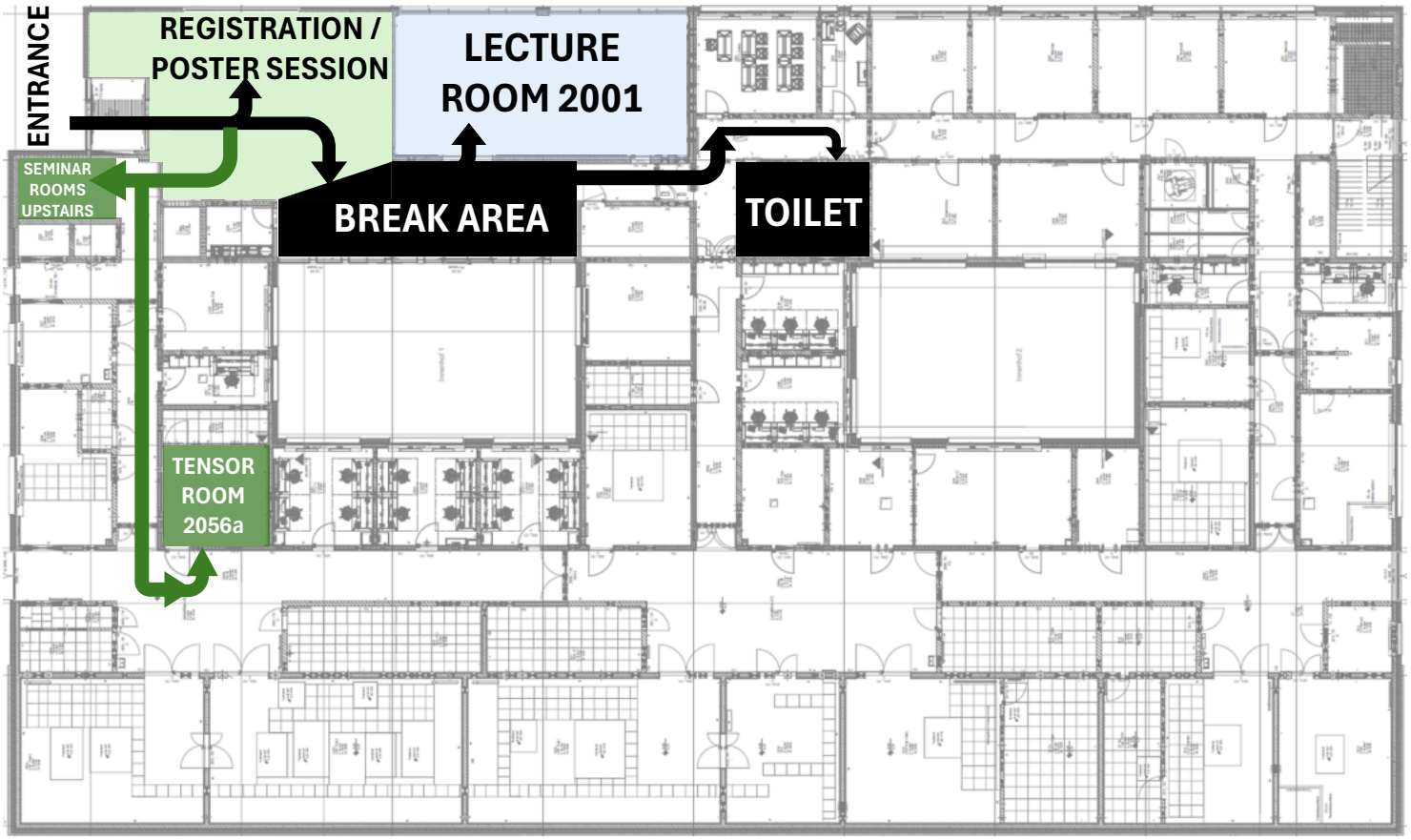

BUILDING 05.2

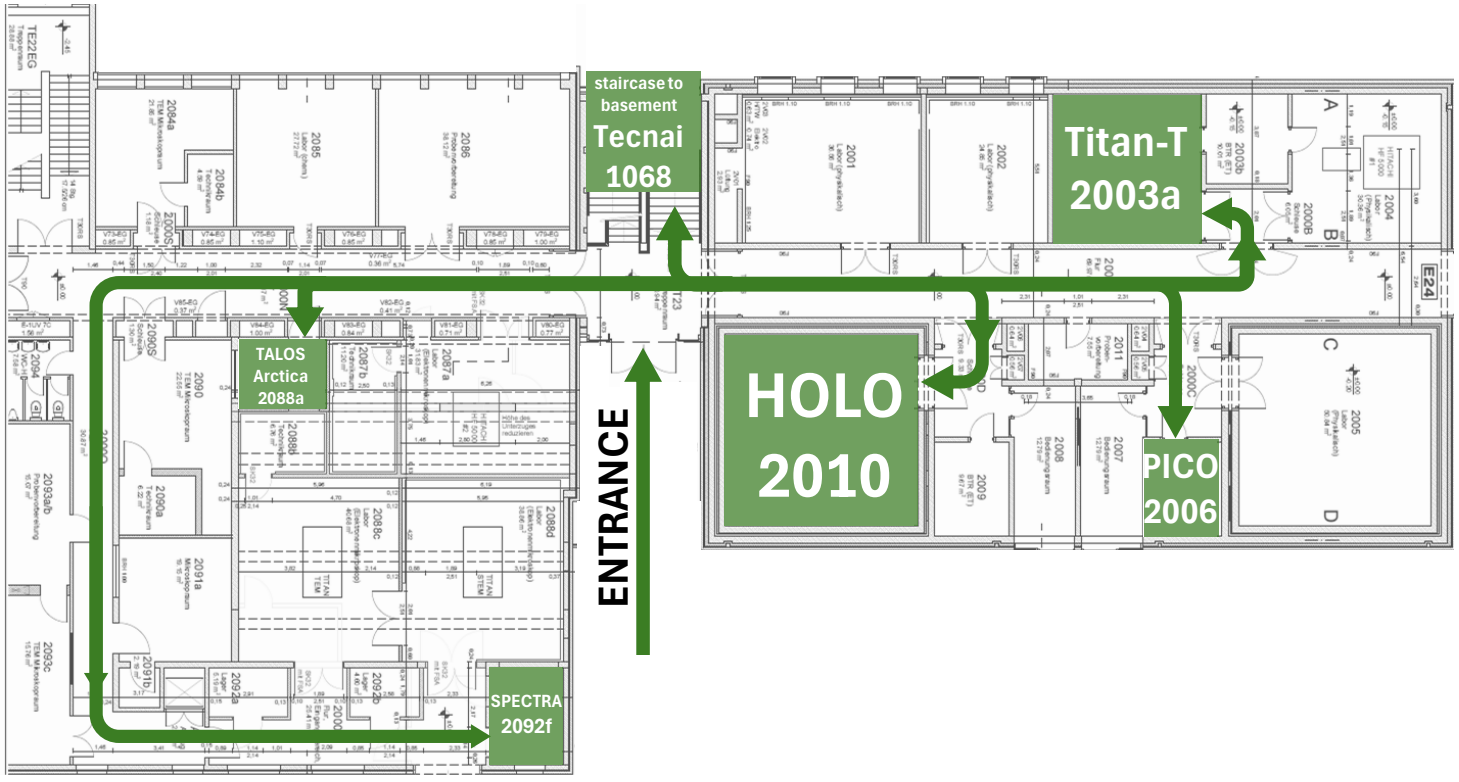

PROGRAM

	MONDAY 02.03. EC BACKGROUND	TUESDAY 03.03. CRYSTALLOGRAPHIC METHODS	WEDNESDAY 04.03. EMERGING DIRECTIONS	THURSDAY 05.03. SCANNING TECHNIQUES & CO	FRIDAY 06.03. SPECIALITIES
08:00 AM - 09:00 AM	08:00 AM Bus transfer to FZJ	08:00 AM Bus transfer to FZJ	08:00 AM Bus transfer to FZJ	08:00 AM Bus transfer to FZJ	08:00 AM Bus transfer to FZJ
09:00 AM - 09:45 AM	Registration Welcome / practical information **Tatiana Gorelik**	Phase problem, Direct methods **Corrado Cuocci**	AI in crystallography **Anders Madsen**	Serial electron diffraction **Sergi Plana Ruiz**	Crystal disorder / diffuse scattering **Ella Schmidt**
09:45 AM - 10:30 AM	Direct and reciprocal space, structure factor **Alexander Eggeman**	Global optimisation methods – simulated annealing & Co. **Corrado Cuocci**	Crystal structure prediction **Jacco van de Streek**	Introduction to 4D-STEM: experimental setup and reconstruction methods **Penghan Lu**	In-situ 3D ED techniques **Joke Hadermann**
10:30 AM - 10:45 AM	coffee	coffee	coffee	coffee	coffee
10:45 AM - 11:30 AM	Crystallographic symmetry, indexing of ED patterns, V-plot, satellites **Paul Klar**	Hybrid iterative methods – SUPERFLIP & Co. **Lukas Palatinus**	Charge density analysis in 3D ED **Lukas Palatinus**	Coherent diffraction imaging **Tatiana Latychevskaia**	Crystallographic phase mapping **Muriel Veron**
11:30 AM - 12:15 PM	Electron scattering: elastic, inelastic, kinematical, dynamical **Mauro Gemmi**	Molecular replacement **Dominique Housset**	Reaching the extremes: ultra-low and ultra-high voltages in electron diffraction **Tatiana Latychevskaia + Paul Klar**	Ptychography **Tatiana Latychevskaia**	ePDF **Ella Schmidt**
12:15 PM - 01:45 PM	lunch	lunch	lunch	lunch	lunch
01.45 PM - 02.30 PM	Instrumental approaches to 3D ED data collection (PED; cRED) **Sergi Plana Ruiz**	**DEMOs / TUTORIALs SESSION 1**	**DEMOs / TUTORIALs SESSION 5**	**DEMOs / TUTORIALs SESSION 7**	Closing
02.30 PM - 03:15 PM	Indexing and integration: peak finding, cylindrical projection, reciprocal space, sectioning **Alexander Eggeman**	**DEMOs / TUTORIALs SESSION 2**	**DEMOs / TUTORIALs SESSION 6**	**DEMOs / TUTORIALs SESSION 8**	02:15 PM bus transfer to Düren train station
03:15 PM - 03.45 PM	coffee	coffee	coffee	coffee	
03:45 PM - 04:30 PM	Assessment of the data quality: symmetry determination, radiation damage, resolution limit **Mauro Gemmi**	**DEMOs / TUTORIALs SESSION 3**	**Poster Session**	**DEMOs / TUTORIALs SESSION 9**	
04:30 PM - 05:15 PM	Kinematical and dynamical refinement **Paul Klar**	**DEMOs / TUTORIALs SESSION 4**		**DEMOs / TUTORIALs SESSION 10**	
05:15 PM - 05:30 PM	Jülich: what are we doing here? **Rafal Dunin-Borkowski**				
05:30 PM - 07:00 PM	Welcome reception / fingerfood	05:30 PM Bus transfer to hotel	05:30 PM Bus transfer to hotel	05:30 PM Bus transfer to dinner	
	07:00 PM Bus transfer to hotel			Dinner Timberjacks Düren	

DEMO DESCRIPTION

1. **Processing 3D Electron Diffraction Data with PETS2**
   This demo introduces the complete workflow for processing 3D electron diffraction data using PETS2. It covers all basic steps, with a particular focus on determining lattice parameters, correcting geometric distortions, and preparing data for dynamical refinement.

2. **3D-ED Data Collection and Processing with XtaLAB Synergy-ED and CrysAlisPro**
   The XtaLAB Synergy-ED is a dedicated electron diffractometer for 3D-ED/MicroED developed by Rigaku and JEOL, with CrysAlisPro as its integrated crystallographic software suite. This demo will cover the full pipeline from instrument control and automated data collection to on- and off-line processing, structure solution, and (dynamical) refinement, using a remote-connected Synergy-ED and example data from Synergy-EDs and general TEMs.

3. **3D Electron diffraction data processing with XDS and XDSGUI.**
   This demonstration introduces the complete workflow for processing three-dimensional electron diffraction (3D-ED) data using XDS, including unit-cell determination, examination of reflection profiles, scaling, space-group determination, and preparation of the data for structure refinement with SHELXL or within the CCP4 suite. Although all required programs can be installed and run locally, we demonstrate the use of a DECTRIS cloud electron diffraction container, in which the necessary software is pre-installed. Once the data have been uploaded, the entire processing workflow can be executed conveniently in the cloud.

4. **4D-STEM Tomography and Precession Electron Diffraction with Tescan TENSOR**
   Tescan TENSOR is a multimodal analytical STEM optimized for electron diffraction, including precession-assisted electron diffraction tomography (PEDT) and 4D-STEM mapping. This demo will present automated acquisition of tomographic 4D-STEM data with built-in fast beam precession, precise crystal tracking, and subsequent analysis for determining crystal parameters and investigating multiple crystal domains.

5. **Automated 3D-ED Data Acquisition with EPU-D**
   EPU-D is a software tool for acquiring electron diffraction data on Thermo Fisher electron microscopes, integrating microscope and camera control into a single, user-friendly interface. In this demo, we will learn how the software operates, how to set up EPU-D presets, how to optimize microscope and specimen conditions, and how to perform basic alignment and data acquisition for 3D-ED (MicroED) experiments.

6. **Continuous-Rotation Electron Diffraction via TEM Scripting**
   This demo presents a simple solution for continuous-rotation electron diffraction based on the GoToWithSpeed function available on many Thermo Fisher microscopes. Using the TEMScripting library embedded in a JavaScript graphical interface, we will demonstrate automated ED data collection with fast cameras, illustrating the complete workflow from setup to acquisition.

7. **TEM Automation and Fast-ADT with Gatan Microscopy Suite**
   Gatan Microscopy Suite provides extensive control of microscopes and Gatan cameras and supports automation via Digital Micrograph scripting. This demo will show how to create simple scripts for routine TEM automation and will conclude with an advanced example illustrating Fast-ADT data collection using a sequential plus precession-based 3D-ED workflow.

8. **Automated Diffraction Data Collection with SerialEM**
   SerialEM is a free, widely used tool for automated TEM data acquisition, compatible with most microscope platforms and detectors. This demo will focus on the use of SerialEM for diffraction imaging and batch acquisition, highlighting the technical aspects of setting up and running automated diffraction experiments.

9. **Automating 3D Electron Diffraction with Instamatic**
   Instamatic is an interoperable Python-based program for automating 3D electron diffraction experiments, supporting routines such as RED, cRED, FastADT, and their serial variants. This session will introduce the software structure and demonstrate the setup, execution, and troubleshooting of selected automated data-collection routines.

10. **Automated MicroED Workflows with Gatan Latitude-D**
    Latitude-D is Gatan's solution for automated continuous-rotation MicroED data acquisition. In this demo, we will show how the software supports the full workflow, from interactive crystal selection and setup of acquisition parameters to real-time monitoring and session management, including low-dose strategies, flexible detector modes, and efficient high-resolution data collection.

DEMO OVERVIEW

No	Description	Location
1	**PETS2** Processing 3D Electron Diffraction Data with PETS2	Building 05.13, ground floor, lecture room 2001
2	**Synergy-ED** 3D-ED Data Collection and Processing with XtaLAB Synergy-ED and CrysAlisPro	Building 05.13, **first floor**, seminar room 3024
3	**XDS** 3D Electron diffraction data processing with XDS and XDSGUI.	Building 05.13, **second floor**, seminar room 4019
4	**TENSOR** 4D-STEM Tomography and Precession Electron Diffraction with Tescan TENSOR	Building 05.13, ground floor, TENSOR room 2056a
5	**EPU-D** Automated 3D-ED Data Acquisition with EPU-D	Building 05.2, ground floor, left TALOS Arctica room 2088a
6	**TEM scripting** Continuous-Rotation Electron Diffraction via TEM Scripting	Building 05.2, ground floor, left SPECTRA room 2092f
7	**Fast-ADT** TEM Automation and Fast-ADT with Gatan Microscopy Suite	Building 05.2, **basement,** Tecnai G2 F20 room 1068
8	**SerialEM** Automated Diffraction Data Collection with SerialEM	Building 05.2, ground floor, right HOLO room 2010
9	**Instamatic** Automating 3D Electron Diffraction with Instamatic	Building 05.2, ground floor, right Titan-T room 2003a
10	**Latitude-D** Automated MicroED Workflows with Gatan Latitude-D	Building 05.2, ground floor, right PICO room 2006

GROUP ROTATION SCHEME

	SESSION 1 Tuesday 3.3. 1:45-2.30 PM	SESSION 2 Tuesday 3.3. 2:30–3:15PM	SESSION 3 Tuesday 3.3. 3:45-4.30 PM	SESSION 4 Tuesday 3.3. 4.30-5.15 PM	SESSION 5 Wed 4.3. 1.45-2.30 PM
1 PETS2	Group 1	Group 10	Group 9	Group 8	Group 7
2 Synergy-ED	Group 2	Group 1	Group 10	Group 9	Group 8
3 XDS	Group 3	Group 2	Group 1	Group 10	Group 9
4 TENSOR	Group 4	Group 3	Group 2	Group 1	Group 10
5 EPU-D	Group 5	Group 4	Group 3	Group 2	Group 1
6 TEM Scripting	Group 6	Group 5	Group 4	Group 3	Group 2
7 Fast-ADT	Group 7	Group 6	Group 5	Group 4	Group 3
8 SerialEM	Group 8	Group 7	Group 6	Group 5	Group 4
9 Instamatic	Group 9	Group 8	Group 7	Group 6	Group 5
10 Latitude-D	Group 10	Group 9	Group 8	Group 7	Group 6
	SESSION 6 Wed 4.3. 2.30-3:15 PM	**SESSION 7** Thu 5.3. 1:45 –2:30PM	**SESSION 8** Thu 5.3. 2:30-3.15 PM	**SESSION 9** Thu 5.3. 3:45-4.30 PM	**SESSION 10** Thu 5.3. 4.30-5.15 PM
1 PETS2	Group 6	Group 5	Group 4	Group 3	Group 2
2 Synergy-ED	Group 7	Group 6	Group 5	Group 4	Group 3
3 XDS	Group 8	Group 7	Group 6	Group 5	Group 4
4 TENSOR	Group 9	Group 8	Group 7	Group 6	Group 5
5 EPU-D	Group 10	Group 9	Group 8	Group 7	Group 6
6 TEM Scripting	Group 1	Group 10	Group 9	Group 8	Group 7
7 Fast-ADT	Group 2	Group 1	Group 10	Group 9	Group 8
8 SerialEM	Group 3	Group 2	Group 1	Group 10	Group 9
9 Instamatic	Group 4	Group 3	Group 2	Group 1	Group 10
10 Latitude-D	Group 5	Group 4	Group 3	Group 2	Group 1

POSTERS

A1 Paulina Indyka
Molecular structure of complex machinery in plant and human complexes
Jagiellonian University, Poland

A2 Sayed Shkeebullah Sadat
Low Energy Electron Holography
Paul Scherrer Institute, Switzerland

A3 Giulia Pia Servetto
Cultured mice brain tissues for the study of the mammalian brain mineralogy
University of Turin, Italy

A4 Jiao Wang
Applying Quantum Crystallography Concepts in 3D Electron Diffraction for Small Bioactive Molecules
University of Warsaw, Poland

A5 Dominik Weh
3D-ED analysis of glycans
Max-Planck-Institute (MPIKG), Germany

B1 Daniel Tchoń
Electron diffraction for everyone: classic and new 3DED protocols in Instamatic
Institute of Physics of the CAS, Czech Republic

B2 Thomas White
CrystFEL for Serial Electron Diffraction
Deutsches Elektronen-Synchrotron, Germany

B3 Zheting Chu
Dispensing Multiple Samples onto One TEM Grid for Electron Diffraction Analysis
Stockholm University, Sweden

B4 Saleh Gorji
Advanced Electron Diffraction Using Gatan Cameras and Latitude-D Automation
Ametek GmbH, Germany

B5 Dean Jannis
AI Auto Tilt for Central Beam and Zone Axis Detection
Thermo Fisher Scientific, Netherlands

B6 Robert Bücker
Overcoming Size Limitations in MOF Research: Structural Elucidation by Electron Diffraction
Rigaku Corporation, Germany

B7 Brandan Clarke
Applications of precession-assisted scanned nanobeam diffraction tomography to sample metrology over large ROIs
Tescan, Czech Republic

C1 Julie Marie Bekkevold
Assessing the Viability of Low-Pixel-Count Detectors for 4D-STEM Phase Retrieval
Thermo Fisher Scientific, Netherlands

C2 Partha Pratim Das
Revealing Nanoscale Structural Variations in Amorphous Materials by ePDF Mapping
NanoMEGAS SRL, Belgium

D1 Seojin Kim
Microscopic Characterization of Evolved Ni Nanoparticle Interface in A-site Deficient Perovskite Titanates
University of St Andrews, United Kingdom
D2 Amoghavarsha Mahadevegowda
A Study of Open Channels in Li-ion Battery Anodes via Scanning Electron Diffraction
University of Cambridge, United Kingdom
D3 Imane Adouar
Synthesis and Characterization of Iron–Magnesium Co-Doped Hydroxyapatite: Structural Insights and Agricultural Implications
USMBA, Morocco
E1 Michal Štulpa
Towards the Simulation of Electron Energy-Loss Spectra
Masaryk University, Czech Republic
E2 Samuel Guimarães
Quantum Crystallographic Methods Applied to the Mineral Titanite ($CaTiSiO_5$)
Federal University of Minas Gerais, Brazil
X Alissa Aarts
Career Options at FZJ
Forschungszentrum Jülich, Germany

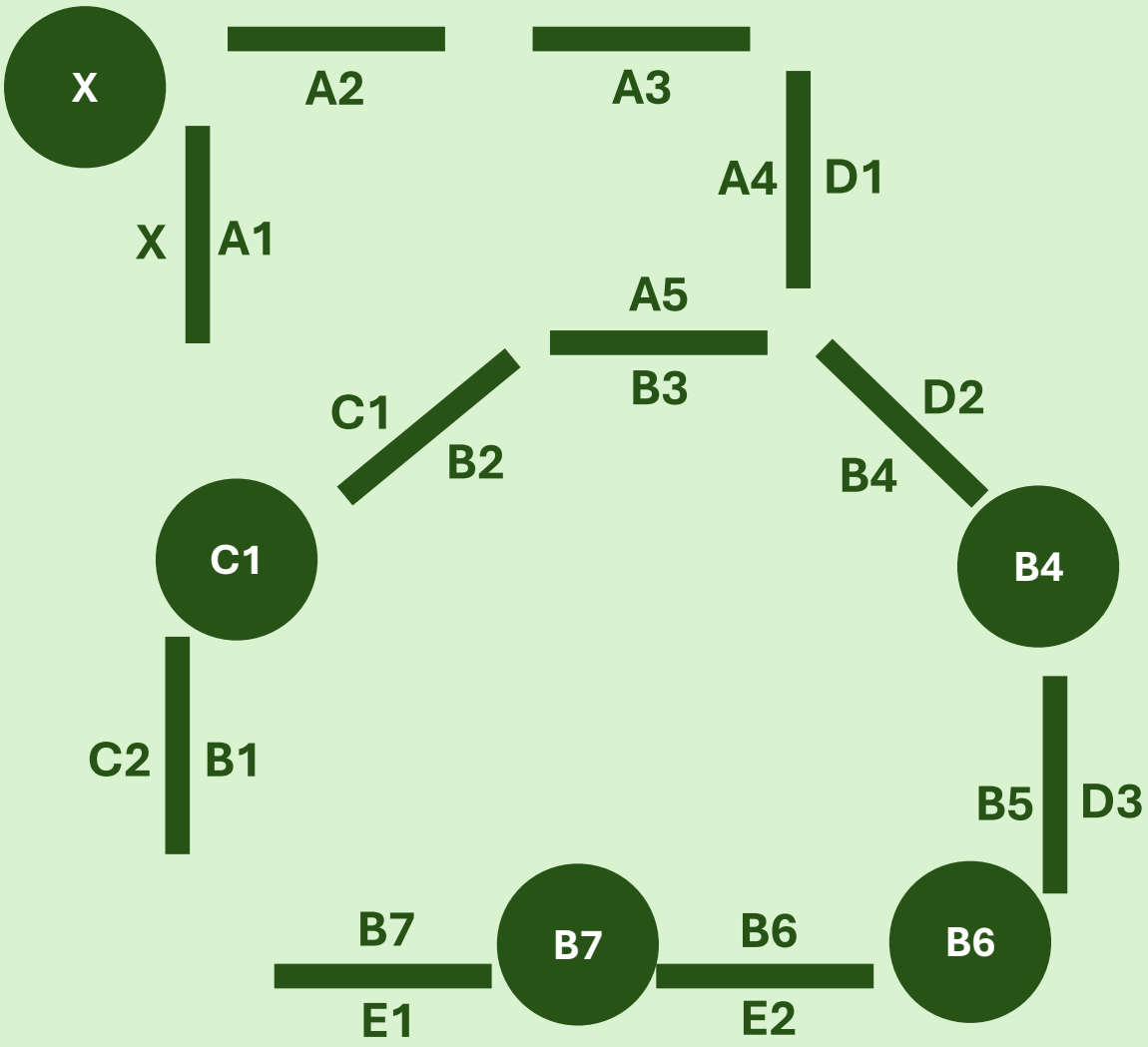

Molecular structure of complex machinery in plant and human complexes

Paulina Indyka[1*], Michał Rawski[1], Marcin Jaciuk[1], Grzegorz Ważny[1,2], Artur Biela[1]

[1]National Synchrotron Radiation Centre SOLARIS, Jagiellonian University, ul. Czerwone Maki 98, 30-392 Kraków, Poland
[2] Doctoral School of Exact and Natural Sciences, Jagiellonian University, Kraków, Poland

[*]paulina.indyka@uj.edu.pl

Plant cells convert solar energy into chemical energy in a process called photosynthesis. The molecular machines that act as power plants, called photosystems, are functionally linked by yet another protein complex, namely cytochrome b_6f [1]. Cytochrome b_6f catalyzes chemical reactions that require quinone molecules as substrates. The structures of cytochrome b_6f described in the published study are resolved at an unprecedentedly high resolution (1.9 Å) and reveal for the first time the position of quinone inside the catalytic site. Intriguing features of the photosynthetic complex machinery in plants were disclosed during its catalytic turnover. The results provide deep mechanistic insights into cytochrome b_6f, one of the key protein complexes in photosynthesis explaining its high efficiency.

The Elongator complex is a conserved multiprotein assembly found in all eukaryotic organisms, including animals, plants, fungi, and protists [2]. It plays a key role in the chemical modification of transfer RNA (tRNA) molecules, which are essential for translation. During this process, tRNAs deliver specific amino acids to ribosomes, enabling their incorporation into newly synthesized proteins.
Cryo-electron microscopy (Cryo-EM) studies have enabled us to determine the biochemical activity and mechanism of action of the Elongator complex. Furthermore, understanding the spatial architecture of this complex allows us to predict how various structural perturbations, such as those caused by mutations, may impair cellular function and affect the entire organism. Notably, mutations in the Elongator complex in humans have been linked to various neurodevelopmental and neurodegenerative disorders, as well as to cancer. These findings highlight the Elongator complex as a promising target for novel therapeutic strategies.

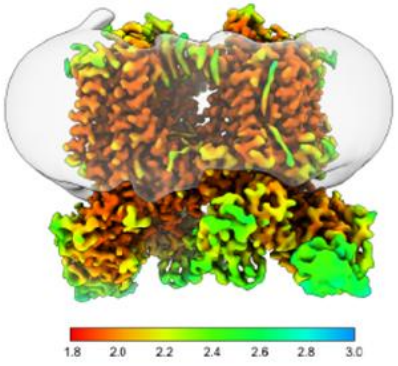

Fig. 1: Cryo-EM of the cyt b_6f local resolution map coded by resolution range [1].

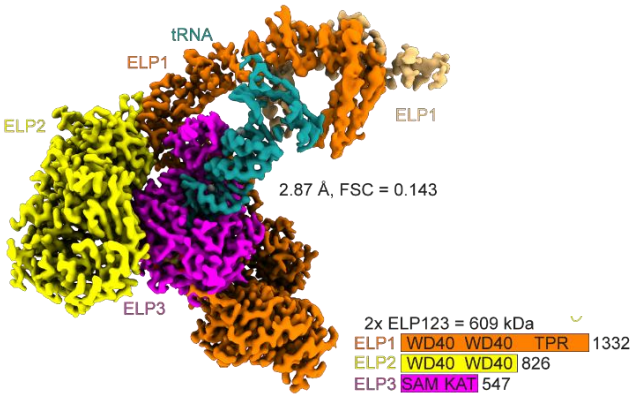

Fig. 2: Human ELP123 cryo-EM structure [2].

References:
[1] S. Pintscher, R. Pietras, B. Mielecki, et al., Nature Plants **10**, 1814-1825 (2024).
[2] NeH. Abbassi, Jaciuk M., Scherf D., et al., Nature Communications **15**, 4094 (2024).

Low Energy Electron Holography

Sayed Shkeebullah Sadat[1,2*], Tatiana Latychevskaia[1,2]

[1]Paul Scherrer Institute, Forschungsstrasse 111, 5232 Villigen, Switzerland
[2]University of Zurich, Physics Department, Winterthurerstrasse 190, 8057 Zurich, Switzerland

[*]sayed.sadat@psi.ch

In-line low-energy electron holography (LEEH) is a lensless and thus aberration-free imaging technique [1,2], which currently achieves sub-nanometer resolution. In LEEH a coherent electron wave originates from a sharp metal tip electron point source. Part of the electron wave is scattered by the sample. The interference between the non-scattered (reference) and scattered (object) waves forms a hologram at the detector plane. The hologram captures both amplitude and phase information of the object wave, and the sample distribution can be numerically reconstructed by the wavefront backpropagation from the hologram to the sample plane, using the Huygens-Fresnel principle. Electrons of low electron energies (20−300 eV) have the advantage of causing negligible radiation damage to biological macromolecules, which makes LEEH a promising tool for imaging individual proteins [3]. Low-energy electrons are also extremely sensitive to local potentials and can image adsorbates with charges less than one elementary charge [4]. These properties make LEEH a promising imaging tool for structural biology or for studying 2D crystals [5].

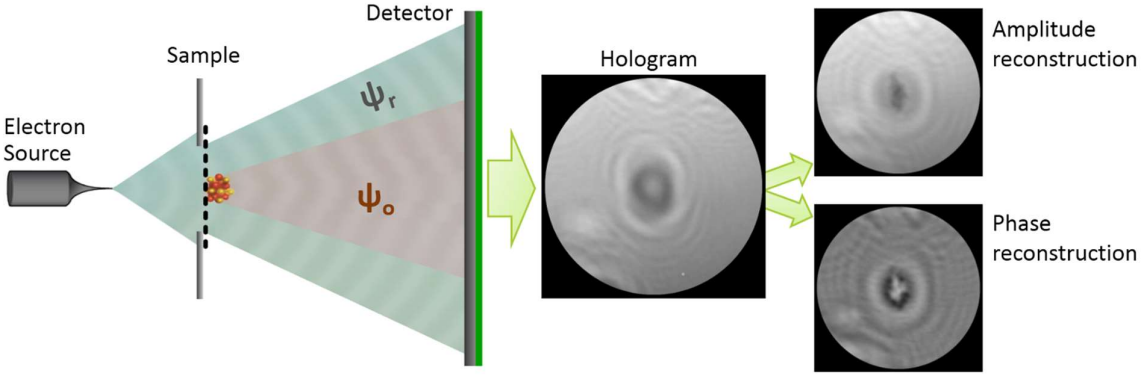

Fig. 1: Principle of in-line low-energy electron holography. [6]

References:
[1] H. W. Fink, et al., *Holography with low-energy electrons*., Phys. Rev. Lett. **65**, 1204–1206, (1990)
[2] T. Latychevskaia, et al., *Holography and coherent diffraction with low-energy electrons: A route towards structural biology at the single molecule level*, Ultramicroscopy **159**, 395–402 (2015)
[4] T. Latychevskaia, et al., *Direct Observation of Individual Charges and Their Dynamics on Graphene by Low-Energy Electron Holography*, Nano Letters **16** (9), 5469-5474 (2016)
[3] J. Longchamp, et al., *Imaging proteins at the single-molecule level*, Proc. Natl. Acad. Sci. U.S.A. **114** (7) 1474-1479, (2017)
[5] M. Lorenzo, et al., *Metal Adsorption and Nucleation on Free-Standing Graphene by Low-Energy Electron Point Source Microscopy*, Nano Letters **18** (6), 3421-3427, (2018)
[6] M. Lorenzo, *Observation of Metal Nucleation on Free-Standing Graphene by Means of Low-Energy Electron Holography*, Dissertation, University of Zurich, (2018)

Cultured mice brain tissues for the study of the mammalian brain mineralogy

Giulia Pia Servetto[1*], Alessandra Passarella[1], Ginevra Mango[1], Filippo Tempia[2], Francesca Montarolo[2], Eriola Hoxha[2], Goran Dražić[3], Ruggero Vigliaturo[1].

[1]Department of Earth Sciencens, University of Turin, Via Valperga Caluso 35, 10125, Turin, Italy
[2] Department of Neuroscience of the University of Turin and Neuroscience Institute Cavalieri Ottolenghi, Regione Gonzole 10, 10043 Orbassano, Italy
[3]National Institute of Chemistry, Hajdrihova ulica 19, 1000 Ljubljana, Slovenia

[*]corresponding author: giuliapia.servetto@unito.it

Abstract

Exogenous mineral phases, including magnetite nanoparticles (NPs), have been found in the human brain after exposure to urban particulate matter. The physicochemical state of these NPs and the mechanisms by which they interact with host tissues remain poorly characterized and understood.

The main goal of this study was to characterize exogenous NPs in cultured mice brain tissues (CMBTs) as a model for a generic mammalian brain environment. These investigations aimed to evaluate the physicochemical alteration of both the NPs surface and bulk mineralogy when exposed to the surrounding biochemical environment.

The nervous system regions selected as CMBTs were the olfactory bulb and the anterior cortex of three separate mices. The CMBTs were treated as following: (i) unexposed to any exogenous NPs (negative control, NC) (ii) exposed for 48 hours to commercial magnetite (Fe_3O_4) NPs (50–100 nm, positive control, PC), and (iii) exposed for 48 hours to magnetic particulate matter taken from tram rails, filtered through a 100 nm mesh (tram dust, TD). The analyses were performed on all sample groups. After the exposure, NC, PC, and TD were split into two subsamples: one chemically fixed and resin embedded for ultramicrotomy, and the other one chemically digested (in NaClO solution at 13%) to extract the NPs of interest. The investigations were carried out using a probe Cs-corrected Scanning Transmission Electron Microscope coupled with Energy Dispersive X-Rays Spectroscopy (HR S/TEM-EDXS) through conventional electron diffraction, STEM-EDXS elemental mapping, and Dual-range Electron Energy-Loss Spectroscopy (Dual-EELS).

Magnetite NPs were detected within the anterior cortex of PC sections. However, HR TEM, diffraction and Dual-EELS analyses were difficult to perform due to sections thickness. NPs were found in both olfactory bulb and anterior cortex of TD sections. The NPs in TD sections were numerically more abundant than magnetite NPs found on PC sections, possibly due to the presence of freshly fractured surfaces resulting from mechanical stress.

Magnetite NPs extracted by chemical digestion from PC were identified and compared with pre-interacted magnetite NPs. Additionally, in chemically digested PC detected NPs showed interplanar distances compatible with goethite (α-FeOOH) and lepidocrocite (γ-FeO(OH)). Tram dust NPs were also identified in the chemically digested TD sample, and comparative analyses with pre- interacted tram rail dust NPs were conducted. The mineralogical phases identified included rutile (TiO_2, found within TD sections as well), and forsterite (Mg_2SiO_4).

APPLYING QUANTUM CRYSTALLOGRAPHY CONCEPTS IN 3D ELECTRON DIFFRACTION FOR SMALL BIOACTIVE MOLECULES

Jiao Wang[1*], Marta Kulik[1], Szymon Sutuła[2], Tomasz Góral[2], Paulina Maria Dominiak[1]

[1]University of Warsaw, Faculty of Chemistry, Biological and Chemical Research Centre, Warsaw, Poland
[2]University of Warsaw, Centre of New Technologies, Warsaw, Poland

[*]j.wang10@uw.edu.pl

Three-dimensional electron diffraction (3D ED, also known as MicroED) has emerged as a powerful technique for determining the crystal structures of nanocrystalline materials. However, the strong interaction between electrons and matter can lead to significant dynamical scattering effects, which may compromise data quality and complicate structural refinement. This study aims to advance quantitative electron density analysis of small bioactive molecules toward the subatomic scale by integrating MicroED within the framework of quantum crystallography. Using adenosine triphosphate (ATP) nanocrystals as a model system, we are developing a comprehensive workflow that includes high-resolution 3D ED data collection, data reduction, and advanced electron density refinement, moving beyond the constraints of the independent atom model (IAM). Continuous-rotation 3D ED measurements under cryogenic conditions yield a reconstructed reciprocal space (Fig. 1), from which the ATP unit cell was determined with lattice parameters a = 6.9 Å, b = 20.8 Å, c = 28.0 Å, and α = β = γ = 90°. Current efforts focus on optimizing sample preparation and performing structure solution and initial refinements—both kinematical and dynamical. Ongoing and future work involves evaluating aspherical atom models for small bioactive molecules and analyzing electrostatic potential distributions to investigate the nature of electronic structure and chemical bonding.. Ultimately, this research aims to enhance the sensitivity and applicability of MicroED for the analysis of biologically relevant materials, thereby extending the structural analysis capabilities of the technique beyond conventional small-molecule benchmarks. This research was funded by National Science Centre, Poland, grant No. 2024/53/B/ST4/02777.

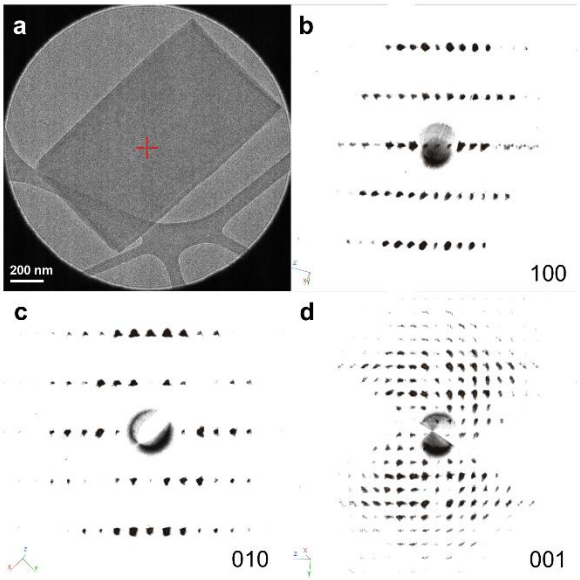

Fig. 1: **TEM image and reconstructed 3D electron diffraction of ATP nanocrystal**. (**a**) Low-resolution TEM image of ATP nanocrystals. (**b–d**) Reconstructed reciprocal-space sections along the [100], [010], and [001] directions from 3D ED data.

3D-ED analysis of glycans

Dominik Weh[1,2*], Yu Ogawa[2] and Martina Delbianco[2]

[1]Freie Universität Berlin, Department of Chemistry and Biochemistry, Arnimallee 22, 14195, Berlin, Germany
[2]Max Planck Institute of Colloids and Interfaces, Department of Biomolecular Systems, Am Mühlenberg 1, 14476, Potsdam, Germany

[*]dominik.weh@mpikg.mpg.de

Life is based on chiral building blocks such as nucleotides, amino acids, and carbohydrates which assemble to form higher-order structures.[1], [2] The specific relationship between mirror-images has been harnessed for protein crystallography.[4] Mirror-image D-proteins can help to determine the crystal structure of native L-proteins through racemic or quasi-racemic crystallization. While this approach enabled structure elucidation of various difficult-to-crystallize proteins, it has yet to be effectively applied to the third pillar of biomolecules: carbohydrates (i.e. oligosaccharides and polysaccharides, a.k.a. glycans). The intrinsic radiation sensitivity of glycans, along with a limited understanding of their crystallization process, has often hindered in-depth investigations of carbohydrates through crystallographic methods.[4] Nevertheless, significant practical knowledge has been accumulated over the past decades, improving the structural analysis of glycans.[4] Recent studies on well-defined synthetic oligosaccharides highlighted that preferential interactions between enantiomers exist.[5], [6] Racemic crystallization of simple monosaccharides further demonstrated the formation of stable racemic crystals.[7] This prompted us to investigate racemic 3D-ED (3D-Electron Diffraction) glycan analysis as a potential technique for enhancing our understanding of glycan structures. Here, we present a study based on racemic mixtures of oligosaccharides with defined length of the structural well-known amylose and of the less-known β-1,6-glucans. For each length both enantiomers were synthesized via AGA (Automated Glycan Assembly), crystallized as racemates and subjected to 3D-ED analysis, revealing aspects of their conformation.

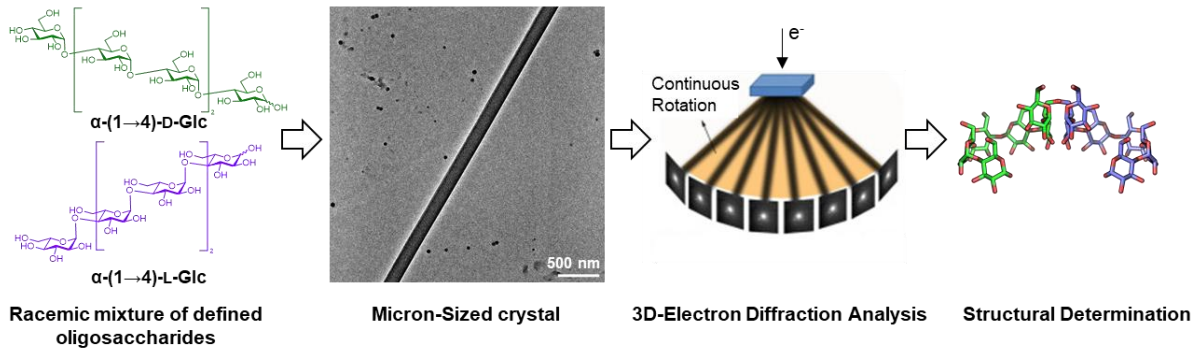

Fig. 1: Illustrative workflow of 3D-ED glycan analysis.

References:

[1] C. J. C Edwards-Gayle, I. W. Hamley, *Organic & Biomolecular Chemistry* **15**, 5867-5876 (2017).
[2] B. Frka-Petesic, T. G. Parton, C. Honorato-Rios, A. Narkevicius, K. Ballu, Q. Shen, Z. Lu, Y. Ogawa, J. S. Haataja, B. E. Droguet, et al., Chemical Reviews, **123**, 12595-12756 (2023).
[3] K. Harrison, A. S, Mackay, L. Kambanis, J. W. C. Maxwell, R. J. Payne, Nature Reviews Chemistry **7**, 383-404 (2023).
[4] Y. Ogawa, J.-L. Putaux, *Frontiers in Chemistry* **10,** (2022).
[5] S. Gim, G. Fittolani, Y. Nishiyama, P. H Seeberger,. Y. Ogawa, M. Delbianco, Angewandte Chemie International Edition **59**, 22577-22583 (2020)
[6] Y. Wu, S. Aslani, H. Han, C. Tang, G. Wu, X. Li, H. Wu, C. L. Stern, Q.-H. Guo, Y. Qiu, et al. Nature Synthesis **3,** 698-706 (2024).
[7] B. Tyson, C. M. Pask, N. George, E. Simone, Crystal Growth & Design **22**, 1371-1383, (2022).

Electron diffraction for everyone: classic and new 3DED protocols in Instamatic

Daniel Tchoń*, Lukáš Palatinus

Department of Structure Analysis, Institute of Physics of the Czech Academy of Sciences,
Na Slovance 1999/2, 182 00 Praha, Czech Republic

*tchon@fzu.cz

With beam characteristics and interaction cross-sections unmatched by photon sources, 3D electron diffraction (3DED) keeps extending crystallography to ever smaller and more challenging targets. While any transmission electron microscope (TEM) can record microdiffraction, the best acquisition strategy depends on the sample: a beam suitable for a mineral sample may rapidly damage an organic one. Likewise, a precise single-crystal protocol will be ill-suited to map phase distribution across many grains.

The simplest 3DED protocol involves rotating the crystal and collecting diffraction stepwise. This rotation ED (RED) can be refined by precessing the beam or acquiring data continuously, as in cRED or Fast-ADT. [1–3] Each variant can be further automated. Through image recognition and clustering, serial 3DED approaches reduce beam damage by distributing the total dose over hundreds to thousands of crystals. [4–6]

As the new 3DED protocols rapidly push the state of the art, they often sacrifice interoperability. In practice, modern 3DED is constrained more by implementation rather than any fundamental limitations. For the wider community, a new experimental protocol is only as valuable as it is applicable across different TEMs.

Here, I present the recent developments in Instamatic – an open-source 3DED data-collection software suite designed for interoperability. Instamatic implements all the protocols mentioned above through a generalised interface that translates commands for different TEMs at runtime. I will showcase recent improvements, including new interfaces, an improved interactive display, refined calibration, and a live emulator. I will discuss a newly developed serial precession-assisted experimental routine that minimises beam damage by replacing direct-space detection and tracking with long continuous scans over the grid. [7]

References:
[1] U. Kolb, T. E. Gorelik, E. Mugnaioli, A. Stewart, Polymer Reviews **50**, 385–409 (2010).
[2] R. Vincent, P. A. Midgley, Ultramicroscopy **53**, 271–282 (1994).
[3] M. O. Cichocka, J. Ångström, B. Wang, X. Zou, S. Smeets, Journal of Applied Crystallography **51**, 1652–1661 (2018).
[4] S. Smeets, X. Zou, W. Wan, Journal of Applied Crystallography **51**, 1262–1273 (2018).
[5] B. Wang, X. Zou, S. Smeets, IUCrJ **6**, 854–867 (2019).
[6] S. Plana-Ruiz, P. Lu, G. Ummethala, R. Dunin-Borkowski, Journal of Applied Crystallography **58**, 1249–1260 (2025).
[7] S. Smeets, B. Wang, E. Hogenbirk, D. Rainer, D. M. Tchoń, Instamatic (2.2.0). Zenodo. https://doi.org/10.5281/zenodo.17857486 (2025).

CRYSTFEL FOR SERIAL ELECTRON DIFFRACTION

Thomas White[1*], Alexandra Tolstikova[1]

[1]Deutsches Elektronen-Synchrotron DESY, Photon Science, Notkestraße 85, 22607, Hamburg, Germany

[*]thomas.white@desy.de

CrystFEL [1] is a software suite for processing serial crystallography data. It was originally created for X-ray free-electron laser (XFEL) experiments, but now extends to data from synchrotron radiation beamlines as well as electron diffraction [2]. At the core of CrystFEL is a program for detecting Bragg peaks, indexing each diffraction pattern individually (with a choice of methods), spot prediction, integration and merging the intensity measurements accounting for physical factors (with a choice of models). A generalised model of detector geometry makes it easy to work with segmented detectors. There are also programs for calculating figures of merit, as well as a fully-featured graphical user interface (GUI) which can interface with the batch system of a high-performance computing cluster. Recently, we have been using CrystFEL as part of a real-time pipeline for automatic data processing, which processes data at over 1000 frames per second with modest computing requirements [3]. Developments specifically for electron diffraction include image readers for electron microscopy data formats, a universal indexing algorithm (“PinkIndexer”) [4], and methods for accounting for lens distortions in the diffraction patterns. These will be based on an algorithm originally devised for high-energy physics, which allows geometrical parameters to be fitted across tens of thousands of diffraction patterns with only a few seconds of calculation [5].

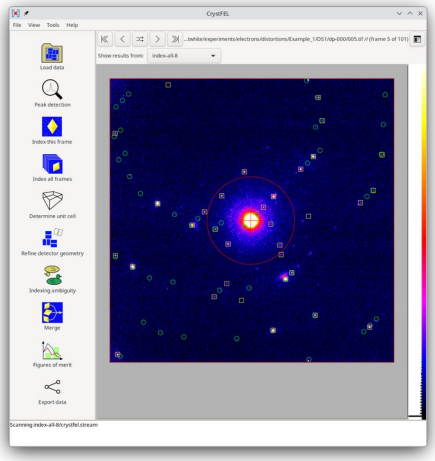

Fig. 1: Screenshot of CrystFEL GUI showing an indexed electron diffraction snapshot.

References:
[1] T. A. White, R. A. Kirian et al., J. Appl. Cryst. **45**, 335-341 (2012).
[2] R. Bücker, P. Hogan-Lamarre, R. J. D. Miller, Front. Mol. Biosci. **8**, 624264 (2021).
[3] T. A. White, T. Schoof et al., IUCrJ **12**, 97-108 (2025).
[4] Y. Gevorkov, A. Barty et al., Acta Cryst. A**76**, 112-131 (2020).
[5] T. A. White, J. Appl. Cryst. in press (2025).

Dispensing Multiple Samples onto One TEM Grid for Electron Diffraction Analysis

Zheting Chu[1], Murat Nulati Yesibulati[2], Xiaodong Zou[1*]

[1] Department of Chemistry, Stockholm University, Sweden
[2] Nanolab, Technical University of Denmark, Denmark

[*] xiaodong.zou@su.se

Electron diffraction (ED), including three-dimensional electron diffraction (3D ED), is widely used for structure determination and phase analysis of small molecules, macromolecules, and functional materials. [1–4] Despite substantial advances in ED data collection and processing, overall throughput remains limited, largely due to slow and manual sample preparation, which remains insufficiently explored. [5] Here, we introduce a human-assisted robotic dispensing approach for ED sample preparation, enabling multiple samples to be arrayed on a single TEM grid (Figure 1). This strategy enables rapid, reproducible preparation of multiplexed samples for ED-based structural analysis and supports up to ~50 samples per grid, depending on solvent properties and grid surface hydrophilicity. Array-based multi-sample deposition on TEM grids has been demonstrated in high-throughput ED applications, such as ArrayED. [6] Building on this concept, we integrate multi-sample dispensing into a general ED analysis workflow without restricting it to a specific ED implementation or sample types. Reliable implementation requires sample pre-treatment strategies to achieve a uniform dispersion. Pre-treatment strategies were evaluated, such as dilution, sonication, and centrifugation. Depending on the compound, samples can be prepared via on-grid crystallization (e.g., tyrosine) or as particle suspensions, with a minimum sample volume of ~20 µL required for dispensing. As a proof-of-principle demonstration, 4 different samples were prepared using the optimized pre-treatment protocol (Figure 2). In a recent trial, 4 TEM grids were prepared within 1.67 hours, each containing 19 different metal–organic frameworks (MOFs). Overall, this work presents a scalable sample preparation strategy that enhances ED throughput and can be readily integrated into existing ED workflows.

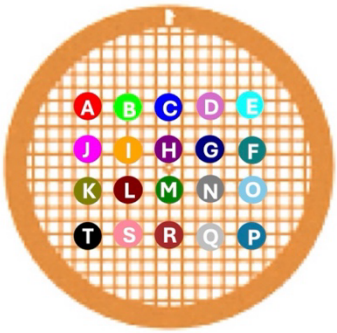

Fig. 1: Schematic illustration of multi-sample dispensing on a single TEM grid

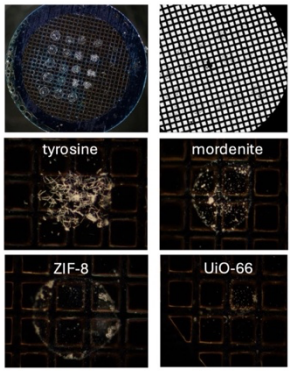

Fig. 2: Proof-of-principle demonstration of multi-sample preparation on a single TEM grid

References:
[1] Yun, Y.; et al. *J. Appl. Cryst*. **47**, 2048–2054 (2014).
[2] Shi, D.; et al. *eLife* **2**, e01345 (2013).
[3] Guo, P.; et al. *Nature* **524**, 74–78 (2015).
[4] Fiorini, G.; et al. *Biophys. J*., in press (2025).
[5] Cichocka, M. O.; et al. *J. Appl. Cryst*. **51**, 1652–1661 (2018).
[6] Delgadillo, D. A.; et al. *ACS Cent. Sci*. **10**, 176–183 (2024).

Advanced Electron Diffraction Using Gatan Cameras and Latitude-D Automation

Saleh Gorji[1*], Fernando Castro[2], Ana Pakzad[2]

[1] Ametek GmbH, EMT (Gatan + EDAX), Rudolf-Diesel-Str. 16, 64331 Weiterstadt, Germany
[2] Gatan, Inc., Pleasanton, CA 94588, United States

[*]saleh.gorji@ametek.com

Electron diffraction is a key technique in TEM for crystallographic analysis of nano- and micro-scale materials. The achievable data quality and experimental flexibility strongly depend on detector performance and acquisition workflows. Recent developments in camera technologies from Gatan, combined with dedicated diffraction automation software, significantly extend the capabilities of modern electron diffraction experiments. Gatan provides a broad portfolio of cameras optimized for diffraction, spanning both scintillator-based and direct electron detection technologies. Scintillator-based cameras such as the ClearView camera and Rio offer a large field of view and robust performance over a wide range of beam conditions. These cameras are well suited for routine diffraction, crystal orientation studies, and applications requiring higher beam currents or increased experimental flexibility. For experiments demanding the highest sensitivity and quantitative accuracy, Gatan's direct electron detection cameras enable diffraction acquisition without a beam stop. Electron counting detectors such as K3, Metro, and Alpine record individual electron events, resulting in superior signal-to-noise ratio, reduced point spread, and high dynamic range. This allows simultaneous detection of intense central beams and weak high-order reflections, supporting continuous-rotation diffraction and three-dimensional reciprocal-space mapping for advanced crystallographic workflows. Representative electron diffraction data acquired using direct electron counting and scintillator-based cameras are shown in Fig. 1, illustrating the complementary diffraction capabilities of Metro, K3, and ClearView detectors. Efficient and reproducible diffraction acquisition is enabled by Latitude-D, a dedicated automation platform designed specifically for diffraction workflows. Latitude-D integrates directly with Gatan cameras to support automated crystal screening, guided diffraction acquisition, session tracking, and parameter optimization. This reduces operator workload, increases throughput, and ensures consistent data quality across large diffraction datasets. Together, Gatan's scintillator-based and direct detection cameras, combined with Latitude-D automation, provide a flexible and scalable solution for electron diffraction, ranging from routine crystallographic measurements to advanced high-throughput and quantitative diffraction experiments.

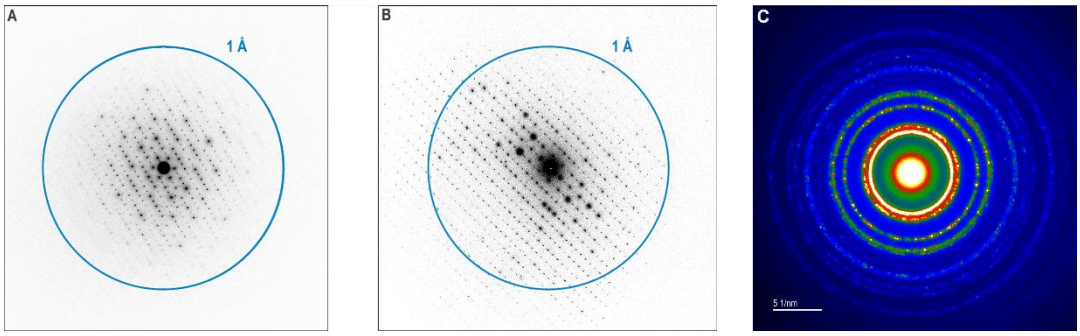

Fig. 1:Electron diffraction patterns acquired without a beam stop using Gatan cameras: (A) ZSM-5 recorded with Metro (5 s exposure, inverted, log scale), (B) ZSM-5 recorded with K3 (1s exposure), and (C) Au nanoparticles recorded with the ClearView.

AI Auto Tilt for Central Beam and Zone Axis Detection

Daen Jannis[1*], Pavel Potocek[1,2], Maurice Peemen[1]

[1]Thermo Fisher Scientific, De Schakel 5, 5651, Eindhoven, Netherlands
[2]Saarland University, Meerwiesertalweg 15, 66123, Saarbrücken, Germany

[*]daen.jannis1@thermofisher.com

Transmission electron microscopes (TEMs) enable imaging at atomic resolution, but their operational complexity and reliance on highly skilled operators significantly limit throughput. One of the most critical and time-consuming steps is crystal alignment, which requires tilting the specimen to align a major zone axis with the electron beam. Recent user-interactive methods have improved efficiency by requiring operator input to identify the central beam and zone axis; however, these approaches still fall short of the automation required for fully self-driving microscopes.

To address this limitation, we present a robust algorithm that automatically identifies both the central beam and the major zone-axis position directly from electron diffraction patterns. While these features are readily recognized by trained users, conventional algorithmic approaches struggle due to the wide variability in experimental parameters such as sample thickness, material type, and acceleration voltage. To overcome these challenges, we employ supervised machine learning to learn the salient features of diffraction patterns and accurately localize the central beam and zone axis across diverse conditions.

We demonstrate the broad applicability of this method across multiple crystallographic systems and experimental parameters, including variations in thickness and convergence angle, and identify the parameter regimes in which the approach is most reliable. Detection results for silicon samples with different thicknesses are shown in Figures 1(a) and 1(b). The method also enables automated alignment in nanoparticle studies, as illustrated by a gold nanoparticle example in Figure 1(c), where the central beam and zone axis are successfully identified.

Overall, this work demonstrates that supervised machine learning can reliably automate a key alignment step in TEM operation. By enabling robust identification of the central beam and zone axis, the proposed approach advances the development of automated and self-driving electron microscopes, substantially improving workflow efficiency and experimental throughput.

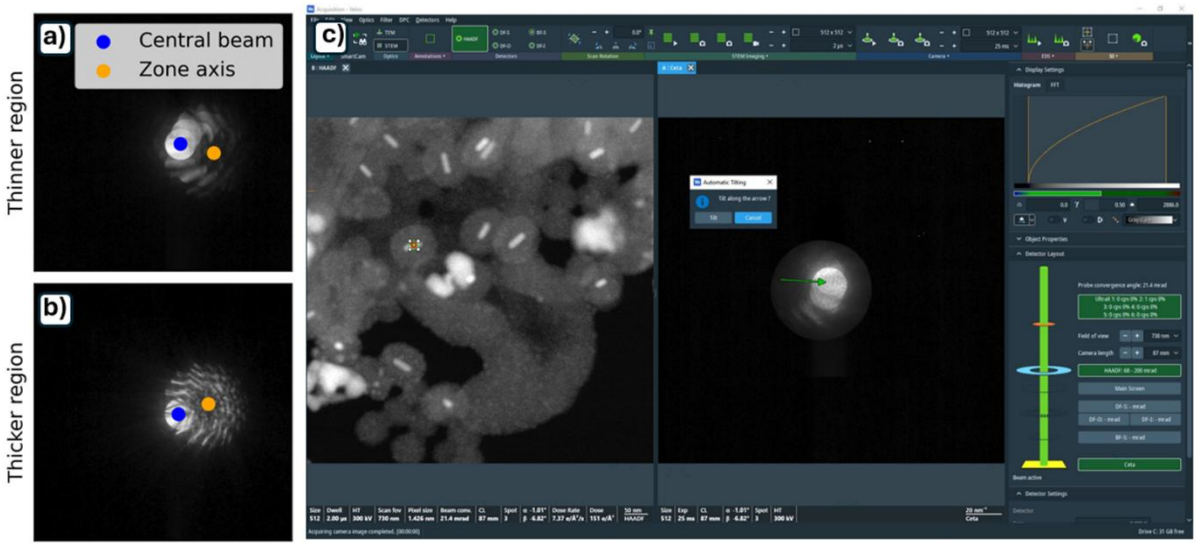

Overcoming Size Limitations in MOF Research: Structural Elucidation by Electron Diffraction

Robert Bücker,[1] Khai-Nghi Truong,[1] Maciej Grzywa,[1] Jakub Wojciechowski,[1] Christian Schürmann,[1] Michał Jasnowski,[2] Mathias Meyer,[2] and Fraser White[1]

[1] Rigaku Europe SE, Neu-Isenburg, Germany
[2] Rigaku Polska, Wrocław, Poland

*robert.buecker@rigaku.com

Since its launch in 2021, the XtaLAB Synergy-ED[1] has produced many structures, with over 600 unique structures from Rigaku labs alone. The majority of those structures have been conducted at ambient temperature, lately with low temperature, particularly cryo-transfer, showing considerable usefulness for preservation of sensitive samples both those sensitive to vacuum and those sensitive to electron beam damage.
Thanks to its compatibility with the existing ecosystem of holders available for TEM instruments, the XtaLAB Synergy-ED is able to provide structural scientists with access to several experiment types already used in X-ray crystallography.
Cryo-transfer specimen holders such as the Gatan ELSA enable the protection of samples before introduction to the vacuum, allowing the study of solvates and other vacuum-sensitive species, [2] in addition to allowing exploration of phase behaviour. Some results from samples for which cryo-transfer proved essential are discussed.
In addition, the Hummingbird Scientific MEMS biasing/heating holder offers the possibility to increase temperature, allowing for exploration of the phase behaviour of materials such as porous materials. Our recent results using single-crystal data from 3D ED/microED electron diffraction on a MOF system, Cu(ta)2 (Hta = 1H-1,2,3-triazole), at room temperature and at 200 °C were compared to a previous study by Grzywa et al.[3] of the same material from 2012 done using SC-XRD and PXRD.

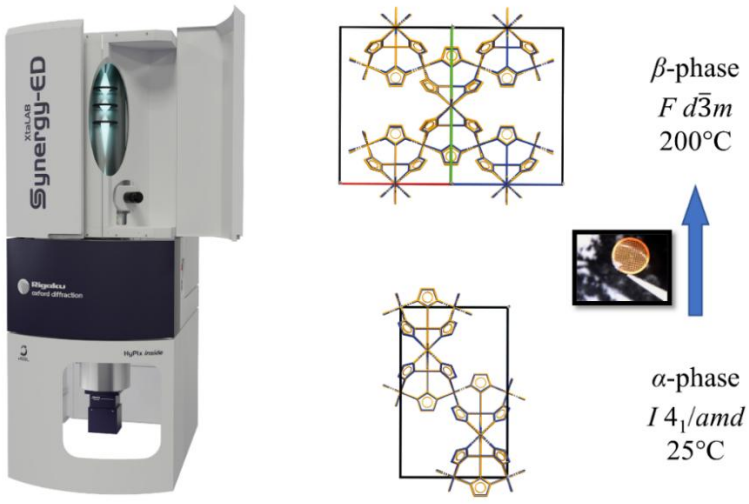

Fig. 1: Overlays of the ambient and high temperature phases of Cu(ta)2 from the XtaLAB Synergy-ED (blue) and the X-ray structures by Grzywa et al. (orange).

References:
[1] S. Ito, F.J. White, et al. *CrystEngComm* **2021**, 23, 8622–8630.
[2] K.-N. Truong, S. Ito, et al. *Symmetry* **2023**, 15(8), 1555.
[3] M. Grzywa, D. Denysenko, et al. *Dalton Trans.* **2012**, 41, 4239–4248.

Applications of precession-assisted scanned nanobeam diffraction tomography to sample metrology over large ROIs

Brendan Clarke[1*], Sara Passuti[2], Philippe Boullay[2], Daniel Nemecek[1], Lukas Palatinus[3]

[1]TESCAN GROUP, Libušina třída 21, 623 00 Brno, Czech Republic
[2]Normandie Université, ENSICAEN, UNICAEN, CNRS, 6 Bd Maréchal Juin, 14000 Caen, France
[3]Institute of Physics of the CAS, Na Slovance 2, 182 00, Czech Republic

[*]Brendan.Clarke@tescan.com

Electron diffraction experiments, such as 3D electron diffraction (3D ED) [1] and 4D-STEM [2], provide structural information on materials at the atomic level. The new dedicated scanning transmission electron diffraction microscope TESCAN TENSOR provides rapid 4D-STEM acquisition and processing that can be uniquely combined with precession-assisted 3D ED tomography [3] to obtain and characterize structural information in crystalline and polycrystalline samples. To illustrate the unique capabilities of TENSOR, we show two techniques for combining 3D ED and per-tilt 4D-STEM to provide structural information that is challenging to acquire with standard diffraction techniques and methods.

First, multimodal electron diffraction is demonstrated here by the mapping a lamella sample of a thermoelectric energy harvesting material [4]. First, the ab initio structural determination of the enargite-type phase is made using precession diffraction tomography. Subsequently, the analysis of the distribution of stannite-type and enargite-type phases is performed, within the same instrument.

Second, the combination of scanned diffraction acquisition and 3D ED can be used for determination of lamella bending and strain relaxation. For every 1° tilt step in a series of 60°, a line scan of a known homogenous structure, Lutetium Aluminum Garnet (LuAG), was acquired in a thinned lamella region. The initial crystal orientation was determined from the first pixel in the scan and used to define a reference. A line acquisition per tilt step was then acquired in the region near the thinned feature of a crystalline lamella sample. Using the tomographic reconstruction of the unit cell for each subsequent pixel in the scan, the lamella bending in this region was measured with greater accuracy than would be possible with qualitative observation of bending contours or template matching.

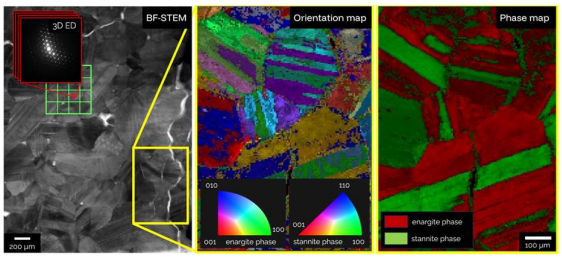

Fig. 1: Multimodal mapping of Cu-rich sulfide ceramic

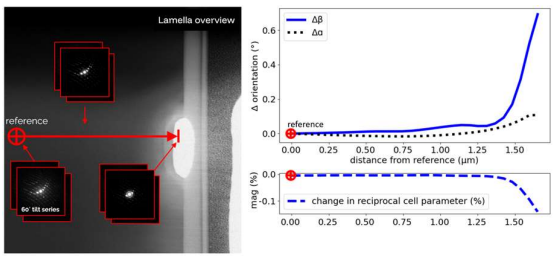

Fig. 2: Scanned 4D-STEM tomography analysis

References:
[1] M. Gemmi, et al. (2019) *ACS Cent.* Sci., **5**: 1315–1329
[2] C. Ophus (2019) Microsc. *Microanal*., **25**: 563–582
[3] A. Eggeman, et al.(2015) *Nat. Commun* **6**: 7267
[4] V.P. Kumar, et al. (2022) *Angew. Chem. Int. Ed.,* **61**: e20221060
[5] E.F. Rauch, M. Veron (2005) *Mat. Sci. Eng. Tech.,* **36**: 552–556
[6] M. Gallagher-Jones, et al. (2020*) IUCrJ,* **7**: 490–499
[7] A.V. Powell, (2019*) J. Appl. Phys.,* **126**: 100901

Assessing the Viability of Low-Pixel-Count Detectors for 4D-STEM Phase Retrieval

Julie Marie Bekkevold[1*], Georgios Varnavides[2,3], Stephanie Ribet[2], Mary Scott[4], Lewys Jones[5], Colin Ophus[6]

[1]Thermo Fisher Scientific, Materials Science Division, Achtseweg Noord 5, 5651GG, Eindhoven, Netherlands
[2]National Center for Electron Microscopy, Lawrence Berkeley National Laboratory, 1 Cyclotron Rd., Berkeley, CA 94720, US
[3]Technische Universiteit Delft, Imaging Physics, Lorentzweg 1, 2628 CJ, Delft, Netherlands
[4]University of California Berkeley, Department of Materials Science and Engineering, Berkeley, CA 94720, US
[5]Trinity College Dublin, School of Physics, College Green, Dublin 2, D02 XN50, Ireland
[6]Stanford University, Department of Materials Science and Engineering, Palo Alto, CA 94305, US

[*]julie.bekkevold@thermofisher.com

Convergent beam electron diffraction (CBED) patterns contain a remarkable density of information about a specimen in scanning transmission electron microscopy (STEM). With the rise of fast, high-dynamic-range pixelated detectors, it has become routine to record a full CBED pattern at every scan position, forming four-dimensional STEM (4D-STEM) [1]. However, only the intensity of the electron wavefunction is detected by these detectors, and any phase information contained in the imaginary part of the electron wavefunction is lost. Several phase-retrieval approaches have been developed to recover this missing information, including integrated center-of-mass (iCOM) [2], tilt-corrected bright-field STEM (parallax) [3], and both direct and iterative ptychography [4,5]. Modern detectors offer extraordinary dynamic range, capturing subtle modulations in the central beam simultaneously with extremely weak high-angle scattering [6]. This richness in recorded intensity enables powerful phase-retrieval techniques. The drawback is data volume: acquiring a full CBED pattern at each probe position incurs substantial read-out overhead, which limits practically achievable scan speeds. This motivates the use of simplified detector geometries such as segmented detectors or low-pixel-count arrays where read-out overhead becomes negligible.

This work examines how far ptychographic phase retrieval can be pushed when using these reduced detector layouts. For iCOM, increasing CBED sampling beyond roughly 16×16 pixels yields diminishing returns because the method fundamentally relies on in-focus probes; analysis of the associated contrast transfer function (CTF) demonstrates this limit [7]. Other phase-retrieval strategies, which can also operate with defocused probes rely more strongly on higher pixel count in the detector since increasing defocus shrinks CBED features. With smaller features in the CBED pattern, the sampling requirement in the detector plane is increased, necessitating more detector pixels for faithful phase reconstruction. In this work, these trade-offs are mapped out and the regimes where simplified detector architecture remains viable for phase retrieval are clarified. The shorter detector read-out times associated with lower pixel number reduce the required dwell time during scanning. This enables faster acquisitions that are compatible with in-situ experiments, where dynamic processes can only be captured if the beam moves quickly enough to capture evolving dynamics.

References:
[1] C. Ophus, Microscopy and Microanalysis **25**, 563 (2019).
[2] I. Lazić, E. G. T. Bosch, and S. Lazar, Ultramicroscopy **160**, 265 (2016).
[3] Y. Yu et al., Nature Methods **22**, 2138 (2025).
[4] H. Yang, P. Ercius, P. D. Nellist, and C. Ophus, Ultramicroscopy **171**, 117 (2016).
[5] Z. Chen et al., Science **372**, 826 (2021).
[6] H. T. Philipp et al., Microscopy and Microanalysis **28**, 425 (2022).
[7] J. M. Bekkevold et al., Elemental Microscopy EM000008 (2025).

Revealing Nanoscale Structural Variations in Amorphous Materials by ePDF Mapping

Partha Pratim Das[1]*, Alejandro Gomez-Perez[1], Evangelos Grivas[1], Stavros Nicolopoulos[1], Simon J. L. Billinge[2], Athanasios S. Galanis[1], Edgar F. Rauch[3], Joaquim Portillo[1], Martijn J. Fransen[1]

[1]NanoMEGAS SRL, Rue Émile Claus 49, bte 9, 1050 Brussels, Belgium
[2]Department of Applied Physics and Applied Mathematics, Columbia University, New York, NY 10027, USA
[3]SIMaP Laboratory, CNRS – Grenoble INP, BP 46, 101 rue de la Physique, 38402 Saint-Martin-d'Hères, France

*partha@nanomegas.com

Understanding the atomic structure of amorphous and nanocrystalline materials requires going beyond conventional diffraction methods, which fail in the absence of sharp Bragg peaks [1]. Electron Pair Distribution Function (ePDF) analysis in a Transmission Electron Microscope (TEM) provides local structural information with nanoscale spatial resolution, minimal sample quantities, and millisecond-scale acquisition times per probe position.

We present a new user-friendly ePDF mapping tool that extracts pair distribution functions from full Scanning Precession Electron Diffraction (SPED) or 4D-STEM datasets. A focused electron probe (~1–10 nm) is scanned with nanometer step sizes, and ePDFs are automatically calculated at every scan position. The resulting maps reveal spatial variations in interatomic distances, peak widths, and intensities, enabling detection of local structural disorder and compositional changes in amorphous and semicrystalline materials [2].

The method complements existing precession-assisted 4D-STEM capabilities such as orientation mapping, phase mapping, strain mapping, and electric field mapping, and can be applied to study semiconductors, glasses, catalysts, amorphous solid dispersions, and polymers. In a recent study presented here, ePDF mapping revealed two distinct amorphous layers in a semiconductor: a Si_xN_y/Si_3N_4 layer (yellow pixels, Fig. 1) with a first peak at 1.65 Å, and a Si_xO_y/SiO_2 layer (green pixels, Fig. 1) exhibiting a slightly shorter first peak at 1.56 Å, likely due to carbon incorporation during fabrication.

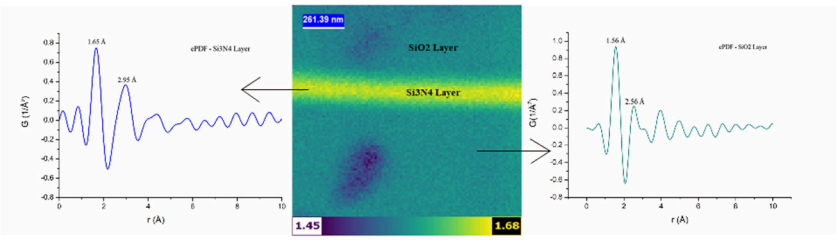

Fig. 1: Peak-position variation map (Å) highlighting Si_3N_4 and SiO_2 layers (center). Left: Si_3N_4 ePDF showing the first two peak positions at 1.65 and 2.95 Å. Right: SiO_2 ePDF showing the first two peak positions at 1.56 and 2.56 Å.

References:

[1] T. Egami, S. J. L. Billinge, *Underneath the Bragg Peaks: Structural Analysis of Complex Materials*, 2nd ed., Pergamon Press, 2012.

[2] Y. Rakita, J. L. Hart, P. P. Das, S. Shahrezaei, D. L. Foley, S. N. Mathaudhu, S. Nicolopoulos, M. L. Taheri, S. J. L. Billinge, Acta Mater. 242 (2023) 118426.

Microscopic Characterization of Exsolved Ni nanoparticle interface in A-site Deficient Perovskite Titanates

SeoJin Kim[1*], John T.S. Irvine[1]

[1]University of St Andrews, School of Chemistry, North Haugh, KY16 9ST, St Andrews, UK

[*]sjk21@st-andrews.ac.uk

When perovskite oxide is exposed at reducing environment at elevated temperature, cation from the structure forms metal nanoparticles on the surface. This phenomenon is known as exsolution. Exsolved perovskite has been the center of interest for its extensive application potential as a catalyst due to its enhanced stability and stronger resistance to agglomeration.[1] The most attractive part of exsolution is that it is possible to tailor the nanoparticles according to need. Previous research shows it is possible to escalate or inhibit exsolution through controlling A-site deficiency, cation doping and reducing environment. To enable tailoring exsolved nanoparticles for optimized use, understanding the mechanism and driving force of exsolution is the key.

Combined research of SEM, EBSD and probe-corrected STEM was carried out to study the relationship between crystal orientation of the perovskite and the morphology of the exsolved nanoparticles. A series of $La_{0.4}Sr_{0.4-x}Ca_xNi_{0.06}Ti_{0.94}O_{3-d}$ where x = 0, 0.2 a d 0.4 were synthesized through solid state process and reduced to exsolve Ni metal nanoparticles. The morphology of Ni nanoparticles exsolved on specific crystal orientations of the perovskite were characterized by Electron Backscatter Diffraction (EBSD) coupled with SEM imaging. The formation of perovskite/nanoparticles interface was observed with probe corrected STEM.

The size and population along with the shape of Ni nanoparticles behaved differently according to the crystal orientation including sphere, trapezoid, rod and triangle shapes. Figure 1 and 2 shows different morphology of the Ni nanoparticles exsolved on grains with different crystal orientation of the same sample. Moreover, Epitaxial interface between nanoparticle and perovskite was observed through STEM images.

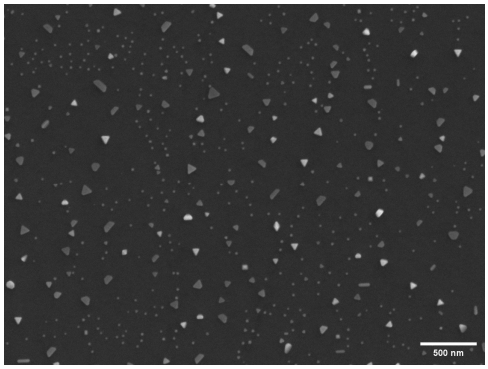

Fig. 1: Ni nanoparticles exsolved on (001) crystal orientation of $La_{0.4}Ca_{0.4}Ni_{0.06}Ti_{0.94}O_{3-d}$ after reduction at 900˚C

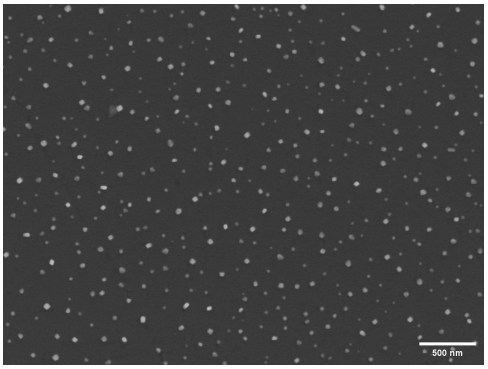

Fig. 2: Ni nanoparticles exsolved on (111) crystal orientation of $La_{0.4}Ca_{0.4}Ni_{0.06}Ti_{0.94}O_{3-d}$ after reduction at 900˚C

[1] D. Neagu, G. Tsekouras, D. N. Miller, H. Menard and J. T. Irvine, *Nat Chem*, 2013, **5**, 916-923.

A STUDY OF OPEN CHANNELS IN LI-ION BATTERY ANODES VIA SCANNING ELECTRON DIFFRACTION

Amoghavarsha Mahadevegowda*, Caterina Ducati

Department of Materials Science and Metallurgy, University of Cambridge, Cambridge, UK
Faraday Institution, Quad One, Harwell Science and Innovation Campus, Didcot, UK

*am2729@cam.ac.uk

Nb-based oxides are increasingly being investigated for their electrochemical attributes, which have shown to significantly improve battery performance [1-2]. These oxides offer stability at high cycling rates coupled with high specific capacities that make them desirable as anodes for Li-ion batteries [1-2]. The source of this relatively high cycling capacity is suggested to originate from an open framework-based structure that facilitates Li-ion diffusion within the Nb-based oxides [3]. These structures are currently being studied by X-ray and neutron diffraction-based techniques. However, such techniques do not offer a view of the local structure within the domain of a crystal that is usually studded with defects, which can only be visualised along a specific crystallographic axis. Moreover, the range over which the local arrangement of atoms stays consistent and essentially demarcates the domain boundaries also varies with composition, which affects Li-diffusion rates within the crystal [1,4-5].

High-resolution transmission electron microscopy can be employed to overcome the shortcomings inherent in X-ray based characterisation techniques. However, the morphology of the oxides - spheres of bundled-up primary particles - make it extremely difficult to image the primary particles and reports are limited to the surface or near-edge of the particles [6-7]. We have used scanning electron diffraction to navigate the entire cross-section of such a sphere, and analysed the patterns using an in-house developed code to identify and image the primary particles. These selected particles were then studied to obtain high-resolution transmission electron microscopy images that revealed the arrangement of cations and defects at a nanoscale, especially in and around the open channels in Nb-based oxides. Our diffraction-based technique has the potential for automation, especially in the new generation of electron microscopes that allow running of custom-made scripts, and hence can enable the study of battery materials at an atomic scale to uncover the underpinning principles of high stability anodes.

References:
[1] T Li et al., Mater. Sci. Eng. R Rep. 2025, 162, 100887
[2] X Zhu et al., ACS Appl. Mater. Interfaces 2018, 10, 23711−23720.
[3] G Li et al., J. Mater. Chem. A, 2013, 1, 12409.
[4] N Takami et al., J. Power Sources 2018, 396, 429–436.
[5] C Kocer et al., Chem. Mater. 2020, 32, 9, 3980–3989.
[6] J Hu, Electrochim. Acta, 331, 2020, 135364.
[7] R Li, Ceram. Int., 45, 9, 2019, 12211-12217.

SYNTHESIS AND CHARACTERIZATION OF IRON–MAGNESIUM CO-DOPED HYDROXYAPATITE: STRUCTURAL INSIGHTS AND AGRICULTURAL IMPLICATIONS

Imane Adouar[1*], Smaiel Herradi[1], Souad Rakib[1], Brahim El bali[1], Mohammed Lachkar[1]

[1] University Sidi Mohamed Ben Abdellah, Faculty of Sciences, Engineering Laboratory of Organometallic, Molecular Materials and Environment, Chemistry Department, Po. Box 1796 (Atlas), 30000 Fez, Morocco

[*]imane.adouar@usmba.ac.ma

Agriculture is the major user of phosphorus fertilizers, accounting for 80-90% of the world demand. With the increasing population, rising demands for bio-energy crops will increase the future demand for chemical fertilizers. However, intensifying the application of these fertilizers will damage the environment, human being health and all living creatures as well. Hydroxyapatite (HAp) is a mineral, $Ca_{10}(PO_4)_6OH_2$, that is the principal storage form of calcium and phosphorus in bones[1]. The nanoparticles of HAp are considered as one of the most important elements in agricultural applications, which can provide phosphorus nutrient [2]. The use of HAp, however, focused on its biomedical applications because of its excellent biocompatibility and bioactivity [3–5], but the agricultural applications are recently taken into consideration.

The aim of this study is to synthesize a novel nanomaterial by co-doping hydroxyapatite with iron and magnesium to use as multi-nutrient soil fertilizer [6], with the goal of enhancing crop productivity and environmental protection through the efficient and minimal use of chemical fertilizers.

References:

[1] I. Cacciotti, Multisubstituted hydroxyapatite powders and coatings: The influence of the codoping on the hydroxyapatite performances, Int. J. Appl. Ceram. Technol. 16 (2019) 1864–1884. https://doi.org/10.1111/IJAC.13229.

[2] S.C. Eugenia, C.T. Mihai, S. Ana-Maria, I. Mariana, S. Marianta-Alexandra, Influence of synthesised hydroxyapatite as a phosphorus fertilizer, Int. Multidiscip. Sci. GeoConference Surv. Geol. Min. Ecol. Manag. SGEM. 19 (2019) 253–260. https://doi.org/10.5593/sgem2019/3.2/S13.034.

[3] S. Herradi, I. Adouar, S. Bouhazma, S. Chajri, M. Khaldi, B. El Bali, M. Lachkar, Sol-gel synthesis of a nanometric hydroxyapatite-silica composite, Mater. Today Proc. 53 (2022) 413–419. https://doi.org/10.1016/J.MATPR.2022.01.393.

[4] S. Herradi, I. Adouar, S. Bouhazma, S. Chajri, M. Khaldi, B. El Bali, M. Lachkar, A physicochemical study of a modified sol-gel derived neodymium-hydroxyapatite, Mater. Today Proc. 53 (2021) 386–391. https://doi.org/10.1016/J.MATPR.2022.01.375.

[5] S. Herradi, I. Adouar, M. Zerrouk, S. Bouhazma, M. El Omari, R. Ouarsal, M. Khaldi, B. El Bali, M. Lachkar, Physicochemical study of magnesium zinc codoped-hydroxyapatite, Moroccan J. Chem. 12 (2024) 1240–1253. https://doi.org/10.48317/IMIST.PRSM/morjchem-v12i3.48113.

[6] I. Adouar, M. Idboumlik, S. Bouhazma, S. Herradi, J.E. Hazm, S. Rakib, B. El Bali, M. Lachkar, Synthesis and characterization of iron and magnesium co-doped hydroxyapatite: effects on cherry tomato fertilization, Moroccan J. Chem. 12 (2024) 1731–1741. https://doi.org/10.48317/IMIST.PRSM/morjchem-v12i4.49810.

TOWARDS THE SIMULATION OF ELECTRON ENERGY-LOSS SPECTRA

Michal Štulpa[1*], Pavel Ondračka[2]

[1]Masaryk University, Department of Condensed Matter Physics, Kotlářská 267/2, 611 37, Brno, Czech Rep.
[2] Masaryk University, Department of Plasma Physics and Technology, Kotlářská 267/2, 611 37, Brno, Czech Rep.

[*]michal.stulpa@gmail.com

As a first step toward the simulation of electron energy-loss spectroscopy (EELS), which is used to probe electronic and collective excitations, the ground state of a given material needs to be computed, e.g. using density functional theory (DFT). Within DFT, a system of Kohn–Sham equations is solved self-consistently. However, the resulting orbitals primarily serve an auxiliary role—to construct the electron density. In order to obtain accurate band structures, the GW approximation within many-body perturbation theory will be employed in the future [1].

Here, we present our first results, namely the band structures and density of states of molybdenum disulfide (MoS_2) in monolayer (ML) and bilayer (AA' stacking) configurations, computed with the software package Quantum ESPRESSO [2]. These results are of interest on their own. We performed appropriate convergence tests and relaxed the crystal cell and atomic positions to prepare the input files. The Perdew–Burke–Ernzerhof (PBE) [3] exchange–correlation functional within the generalized gradient approximation was adopted. For ML MoS_2 we compared two norm-conserving PBE pseudopotentials (PPs): a scalar relativistic (SR) and a fully relativistic (FR). While the SR PP produced an indirect band gap, the FR PP calculation with spin–orbit coupling produced a direct band gap at the K point of the first Brillouin zone. In the bilayer case, with explicit Grimme's DFT-D3 van der Waals correction, an indirect band gap between Γ and K is observed, which highlights an important property of MoS_2 multilayers.

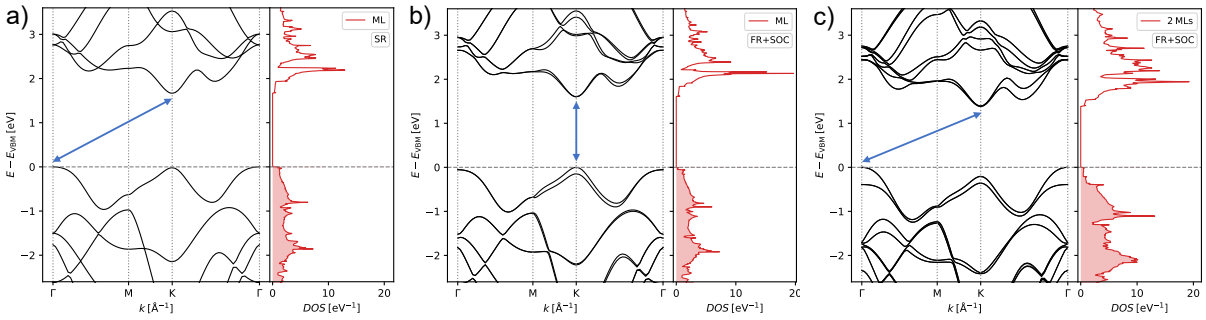

Fig. 1: Simulated band structures and density of states (DOS) of monolayer (ML) and bilayer (2 MLs) MoS_2 plotted relative to the valence band maximum (VBM). Band gaps are indicated by blue arrows. *a)* In the monolayer case, the use of a scalar relativistic (SR) pseudopotential (PP) leads to an indirect band gap of 1.67 eV while *b)* the use of a fully relativistic (FR) PP and spin-orbit coupling (SOC) results in a direct band gap of 1.60 eV at the K point of the first Brillouin zone. *c)* In bilayer MoS_2, when SOC and van der Waals corrections are included, an indirect band gap of 1.38 eV between Γ and K points is observed.

References:
[1] A. Paták *et al.*, Physical Review B **111**, 125113 (2025).
[2] P. Giannozzi *et al.*, Journal of Physics: Condensed Matter **29**, 465901 (2017).
[3] J. P. Perdew, K. Burke, and M. Ernzerhof, Physical Review Letters **77**, 3865 (1996).

QUANTUM CRYSTALLOGRAPHIC METHODS APPLIED TO THE MINERAL TITANITE ($CaTiSiO_5$)

Samuel P. Guimarães*, Bernardo Lages Rodrigues

Federal University of Minas Gerais, Chemistry Department, 2 Mario Werneck St.,31270-901, Belo Horizonte, Brazil

*samuelpguimaraes@ufmg.br

Charge density analysis is one important topic of crystallography research. The possibility of studying the electron density of crystal structures from experimental data can yield interesting insights from the perspectives of structural chemistry, materials science, pharmaceutical and drug chemistry, among other applications [1]. Due to this versatility, a large spectrum of crystalline substances is studied across organic, metal-organic, and inorganic structures. Mineral structures are relevant to both geology and materials science, and they exhibit a great structural and chemical variety, making them interesting in the context of structural chemistry and charge density analysis.

In this work, a natural sample of the mineral titanite ($CaTiO_5$) was studied using two quantum crystallographic methods: the Multipolar Model by Hansen-Coppens (MM) [2] and the Hirshfeld Atom Refinement (HAR) [3,4] using high-resolution single-crystal X-ray diffraction data. A theoretical chemistry approach was also employed, with DFT calculations performed to compare the results with the experimental data. In all models, a topological analysis was performed using the Quantum Theory of Atoms in Molecules by Richard Bader [5].

It was possible to observe the charge transfer from the calcium, titanium, and silicon to oxygen, and observe the ionic character of these bonds in the deformation maps. The charges obtained were chemically reasonable in all models, considering the monopole populations in MM refinement ($q_{Monopole}$) and the Bader charges in the topological analysis (q_{MM}, $q_{HAR,}$ and q_{DFT}). For Ca were obtained $q_{Monopole}$=+1.80, q_{MM}=+1.65, q_{HAR}=+1.60, q_{DFT}=+1.61. For Ti $q_{Monopole}$=+3.58, q_{MM} =+3.21, q_{HAR}=+2.30, q_{DFT}=+2.27. For Si $q_{Monopole}$=+2.97, q_{MM}=+3.21, q_{HAR}=+3.19, q_{DFT}=+3.14. And the average O charges were $q_{Monopole}$=-1.65, q_{MM}=-1.63, q_{HAR} =-1.37, q_{DFT} =-1.36. In all cases, charge neutrality was obeyed, and in the topological analysis, the atomic volumes add up to the cell volume of the crystal.

References:

[1] Koritsanszky, Tibor S., and Philip Coppens. "Chemical applications of X-ray charge-density analysis." Chemical reviews 101.6 (2001): 1583-1628.

[2] Hansen, Niels K., and Philip Coppens. “Testing Aspherical Atom Refinements on Small-Molecule Data Sets.” Acta Crystallographica Section A: Foundations and Advances 34 (1978): 909–921.

[3] Jayatilaka, Dylan, and Birger Dittrich. "X-ray structure refinement using aspherical atomic density functions obtained from quantum-mechanical calculations." Foundations of Crystallography 64.3 (2008): 383-393.

[4] Capelli, Silvia C., et al. "Hirshfeld atom refinement." IUCrJ 1.5 (2014): 361-379.

[5] Bader, Richard FW. "Atoms In Molecules: A quantum theory." Clarendon: Oxford, UK 556 (1990).

Career Opportunities Forschungszentrum Jülich

Alissa Aarts[1]

[1]Forschungszentrum Jülich, HR, Wilhelm-Johnen-Straße, 52428, Jülich

[*]a.aarts@fz-juelich.de

Conducting research for a changing society: This is what drives us at Forschungszentrum Jülich. As a member of the Helmholtz Association, we aim to tackle the grand challenges of our times. How can we utilize the potential of artificial intelligence for society and science? How can we decode the human brain? How can we make a success of the energy transition and mitigate the effects of climate change? And how can we facilitate the transition to a sustainable economy in regions affected by structural change? Come and work with us at our scientific institutes, administration, or in research management alongside around 7,700 colleagues from almost 110 countries at one of Europe's biggest research centres and help make a contribution to solving societal challenges. Help us to shape change!

We offer our employees an international and interdisciplinary working environment on an attractive research campus as well as exciting and varied responsibilities. Cooperation is characterised by collegiality, which thrives on the commitment and enthusiasm of all. It is reflected in appreciative interactions, responsible leadership, reliability, and the willingness to constantly learn from each other.

With our family-friendly corporate policy, we support all employees in reconciling work and care. Flexible working hours, the possibility of mobile working, support with childcare and care for relatives as well as counselling in individual life situations are instruments we rely on. We support employees and their families who come to us from abroad with targeted services such as our International Advisory Service.

Every year, we have more than 1,000 openings for apprentices, university students, doctoral researchers, research assistants, postdocs and management positions in science, as well as for young professionals and experienced professionals in science, technical and administrative infrastructure and science management.

We welcome applications from people with diverse backgrounds, e.g. in terms of age, gender, disability, sexual orientation / identity, and social, ethnic and religious origin. A diverse and inclusive working environment with equal opportunities in which everyone can realize their potential is important to us.

For more information on career opportunities, visit www.fz-juelich.de/careers.
Learn more about the values, mission and vision of Forschungszentrum Jülich in our mission statement: https://go.fzj.de/leitbild

Figure 1: Abstract Illustration of central research elements at Forschungszentrum Jülich

The organizers gratefully acknowledge support of WiSE-Cryst 2026 by these enterprises and organizations.

Ernst Ruska-Centre for Microscopy and Spectroscopy with Electrons
Forschungszentrum Jülich GmbH
www.er-c.org